Global pulsations of intraplate magmatism through the Cenozoic

Rolf Mjelde[1]*, Paul Wessel[2], and R. Dietmar Müller[3]
[1]DEPARTMENT OF EARTH SCIENCE, UNIVERSITY OF BERGEN, ALLÉGATEN 41, 5007, BERGEN, NORWAY
[2]SCHOOL OF OCEAN AND EARTH SCIENCE, UNIVERSITY OF HAWAII AT MANOA, HONOLULU, HAWAII 96822, USA
[3]SCHOOL OF GEOSCIENCES, UNIVERSITY OF SYDNEY, BUILDING F05, SYDNEY, NSW2006, AUSTRALIA

ABSTRACT

A review of Earth's most significant intraplate Cenozoic hotspots with regard to variations in magmatic productivity through time indicates periodicities with a dominant period of ~10 m.y. and a secondary period of ~5 m.y. It is unlikely that the observed global variations in magmatic productivity can be explained by differences in lithospheric thickness, intraplate stresses, and/or interaction with oceanic spreading ridges. The majority of hotspots are located near the edges of the lower-mantle low-velocity anomalies under Africa and the central Pacific, suggesting that hotspots are the surface expressions of mantle plumes originating from the deepest mantle. It is postulated that the apparent co-pulsations in magmatism result from global fluctuations in core-mantle interaction, involving periodic heating of Earth's core and subsequent increases in global plume activity from the edges of the lower-mantle anomalies.

INTRODUCTION

Hotspot chains result from the drift of a lithospheric plate over a (more) stationary area of mantle upwelling (e.g., Wilson, 1963). It is well known that the magmatic production related to many of the long-lived hotspots on Earth varies with time, e.g., Hawaii (Van Ark and Lin, 2004). For individual hotspots, such fluctuations may be associated with lithospheric thickness variations (White, 1993), variable decompression melting during rifting (van Wijk et al., 2001), plate tectonic reorganizations (Knesel et al., 2008), interaction with spreading ridges (Vogt, 1976), solitary waves in plume conduits (Ito, 2001), and plume separation effects at mantle discontinuities (Bercovici and Mahoney, 1994).

In a recent paper, Mjelde and Faleide (2009) presented evidence indicating that the Hawaiian and Icelandic hotspots co-pulsate with a frequency of ~15 m.y. If confirmed, this hypothesis might provide new insight into the interplay between mantle dynamics and plate tectonics, and possibly also in core-mantle interactions.

The present paper represents a review of Earth's most significant intraplate Cenozoic hotspots (omitting the Holocene) with regard to variations in magmatic productivity through time. The study includes all major hotspots that, according to Courtillot et al. (2003), were related to mantle plumes originating from the core-mantle boundary (Hawaii, Louisville,

Easter, Iceland, Afar, La Réunion, Tristan), in addition to other Pacific hotspots (Galápagos, Samoa, Ontong Java, Tasmantid, Society), Atlantic hotspots (Azores, Madeira, Canary Islands, Cape Verde, St. Helena), Kerguelen from the Indian Ocean, as well as Afar-Kenya, Yellowstone, and European magmatism (Fig. 1; Table 1). We did not include magmatism related to normal seafloor accretion or subduction. The various mechanisms for hotspot pulsations listed here will be considered in light of our review of observations.

METHOD

Wide-Angle Seismic Data

White (1993) argued that the analysis of crustal thickness estimates obtained from the modeling of wide-angle seismic data represents the most reliable method for calculating magmatic production rates. When applying this method to oceanic crust, the hotspot production rate is obtained by subtracting the (estimated) thickness of the crust formed under normal oceanic accretion from the (observed) total thickness. This method has been extensively used in the North Atlantic with regard to the production from the Icelandic hotspot (e.g., Holbrook et al., 2001).

The method is also applicable on land, but must there be applied with caution. Magmatism in continental lithosphere is a function of factors like craton age, rheology, strain rates, and rifting history, and age estimates of continental, lower-

crustal underplates are uncertain (e.g., Mjelde et al., 2009).

Bathymetry and Gravity Data

On oceanic crust, the surface manifestation of a hotspot is associated with (1) a volcanic chain expressing an age progression as the tectonic plate drifts across the mantle anomaly, and (2) a large positive depth anomaly hundreds of kilometers across, called a swell (e.g., Crough, 1983). The swell is considered to be a consequence of the upwelling mantle, and is therefore commonly used as a parameter in studies of hotspot strength (e.g., Courtillot et al., 2003). However, this parameter is inadequate to study the history of hotspot chains because the amplitude of the swell decays due to lithospheric cooling and the growing distance between the mantle plume and older portions of a volcanic hotspot chain. The volcanic material along the hotspot chain is not influenced by this cooling, and thus can be used as a direct record of the volcanic activity. Vidal and Bonneville (2004) and Adam et al. (2005, 2007) used a combination of the production rate of volcanic material (Q_v) and the swell flux (Q_s) to estimate the evolution of the Hawaiian and Tristan hotspots, respectively. Such studies use available bathymetry, sediment thicknesses, and seafloor ages in order to correct for thermal subsidence and sediment loading. It is generally assumed that the volcanic loading is supported by an elastic lithosphere for which elastic thickness is deduced from the age of the crust at the time of loading (Watts et al., 1975).

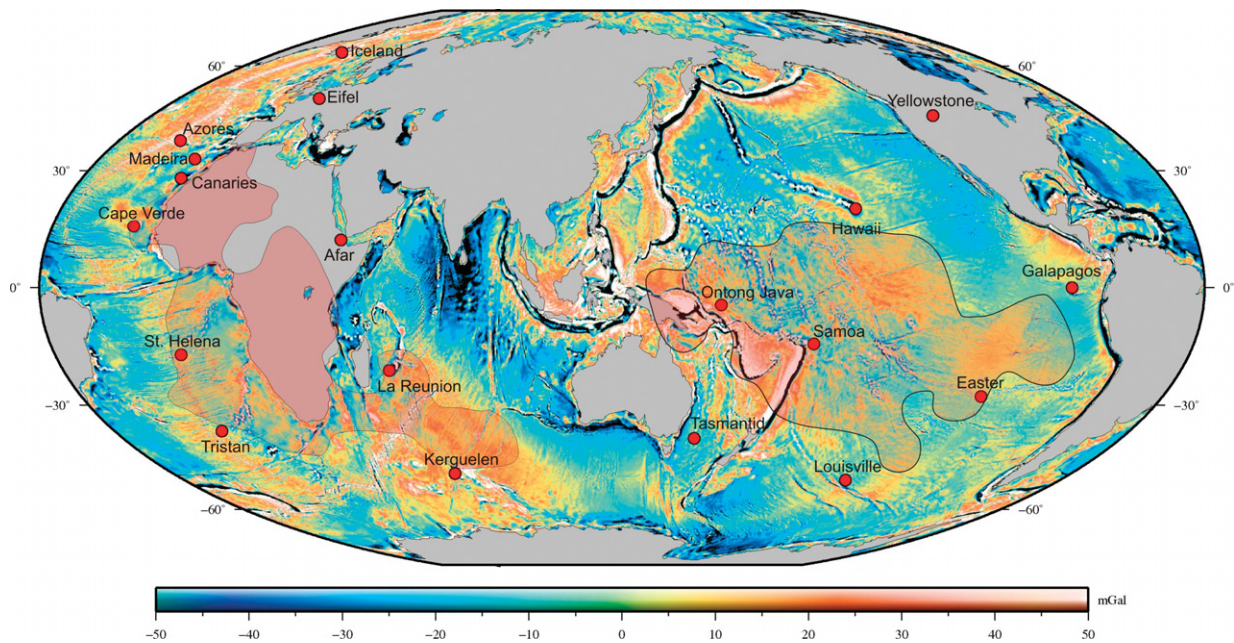*Corresponding author e-mail: Rolf.Mjelde@geo.uib.no.

Figure 1. Ocean gravity map with present-day localization of studied hotspots indicated by red dots. The Eifel hotspot is shown as example of the widespread European magmatism (Lustrino and Wilson, 2007). See Hillier (2007) for location of Pacific seamounts. Shaded areas show the locations of the Pacific and African lower-mantle shear wave anomalies (2850 km depth; Ritsema et al., 1999). Color scale is free-air gravity in mGal.

TABLE 1. GEOGRAPHICAL COORDINATES OF THE PRESENT-DAY LOCATION OF HOTSPOTS INCLUDED IN THE PRESENT STUDY

	Longitude	Latitude
Iceland	16.5°W	64.4°N
Tristan da Cunha	12.0°W	37.0°S
Cape Verde	17.0°W	14.0°N
Canary Islands	17.0°W	28.0°N
Madeira	17.0°W	33.0°N
Azores	28.0°W	38.0°N
Eifel	7.0°E	50.0°N
Afar	42.0°E	12.0°N
Hawaii	155.0°W	20.0°N
Louisville	138.1°W	50.9°S
Galápagos	91.0°W	0.0
Samoa	169.6°W	14.2°S
Ontong Java	160.0°W	9.0°S
Easter	110.6°W	27.8°S
La Réunion	55.0°E	21.0°S
Kerguelen	63.0°E	49.0°S
Yellowstone	111.0°W	45.0°N
St. Helena	10.0°W	17.0°S
Tasmantid	156.0°E	39.0°S

Note: The location of the Eifel hotspot is shown as an example of the widespread European magmatism (Lustrino and Wilson, 2007).

Age Estimates

Some hotspots express long histories of direct interaction with oceanic spreading ridges. One example is the Icelandic hotspot, which has interacted with the North Atlantic spreading ridge since continental breakup at ca. 53 Ma

(e.g., Mjelde et al., 2008). In such cases, the hotspot production rate can be directly linked to the corresponding age of oceanic magnetic anomalies (Cande and Kent, 1995).

However, not all of the magmatism related to the Icelandic hotspot has interacted with the Mid-Atlantic spreading ridge. Breivik et al. (2008) documented a Miocene magmatic pulse well east of the spreading ridge and dated the pulse by use of the induced regional sedimentary unconformity.

Volcanic samples are usually dated radiometrically by the incremental heating $^{40}Ar/^{39}Ar$ technique. This technique is more reliable and accurate than the K-Ar and total fusion $^{40}Ar/^{39}Ar$ techniques commonly used earlier, since these methods cannot be used to discriminate between fresh and altered rock samples (Koppers et al., 2004).

Since radiometric estimates of seamounts are sparse, their age may be inferred indirectly. This is achieved by calibrating lithospheric strength against the age of the dated seamounts, and subsequently using this relationship to estimate the age of other seamounts (Hillier, 2007).

Integrated Approach

As outlined here, the variation of magmatism along a marine hotspot chain can be modeled either by use of wide-angle seismic or bathymetric/gravimetric data. Areas with thicker crust cor-

respond to excess magmatic productivity; their ages are found by use of dated magnetic anomalies or radiometric ages from nearby seamounts. Where geophysical data are not available, the age of magmatic pulses is constrained from dating of seamounts only. It is thus assumed that the generation of seamounts corresponds to periods of increased magmatic activity, an assumption confirmed, for example, by the Hawaiian hotspot (Van Ark and Lin, 2004). For hotspots on land, the procedure is similar: wide-angle seismic data are used when available, and voluminous magmatic events are dated radiometrically.

In our search for periods of increased magmatic activity, we have included all relevant literature concerning the hotspots studied (Table 1). The different hotspots have been investigated using a combination of the methods described here, i.e., not every hotspot has been studied by all available methods. The actual methods used for each individual hotspot are listed in Table 2. More than half of the hotspots have been studied by wide-angle seismics, but only three have been analyzed by use of bathymetry/gravimetry. Crust along all hotspots has been dated radiometrically, and magnetic anomalies have been used for dating for approximately half of the hotspots.

Ideally, data for all investigated hotspot chains should have been reanalyzed using a standard approach. However, such a study represents a formidable undertaking, and as a first

measure, we will here analyze the published findings of others from these chains. We recognize that differences in methodology, data quality, and data types will affect our conclusions.

We define magmatic pulses as periods with magmatic productivity (in m³/s) at least 50% higher than the background value for a specific hotspot. The same magmatic peak might be assigned a slightly different age (± a few m.y.) by various authors. In such cases, we refer to the average age (Ma), and we list the studies included in the averaging for each individual pulse. We also use the average age when two reported peaks are closer than 3 m.y., implying that our study cannot resolve periods smaller than 5 m.y. The model step size is 1 m.y.

RESULTS: MAGMATIC EVENTS FOR THE STUDIED HOTSPOTS

We will in the following describe the variation in production for all studied hotspots (Table 1). We have chosen to indicate the peak of reported relatively short-lived (<5 m.y.) pulses of increased magmatism. For longer events (>5 m.y.) of unknown duration, we have marked the onset of the magmatism. One exception concerns the Icelandic hotspot, where the breakup anomaly appears to have lasted longer than 20 m.y. We have chosen to indicate the peak magmatism at breakup (ca. 53 Ma) for this event, since it is well dated. Furthermore, for the long Miocene event on the Walvis Ridge, we have indicated both its marked onset at ca. 23 Ma and its peak at ca. 10 Ma (Adam et al., 2007). We recognize that including both the start of events and magmatic maxima might imply that several processes involving increase in magmatism have been mixed. However, this procedure is necessary in order to ensure that the results are statistically significant. The length of long-duration events influences the production estimates, but not the timing.

Iceland

Based on published results from the North Atlantic, Mjelde and Faleide (2009) estimated the total Cenozoic volumetric production from the Iceland hotspot (Fig. 2) at 22.1 × 10⁶ km³. They found that the magmatic production varied significantly with time, with a clear maximum of 55.5 m³/s around continental breakup at ca. 53 Ma. The lowest production is estimated at 4 m³/s, increasing to 7 m³/s at ca. 23 Ma. Two other pulses with increased activity are found around 40 Ma and in the late Miocene (ca. 8 Ma). The average Cenozoic magmatic production rate is estimated at ~12 m³/s, and since 23 Ma, the rate has been ~8 m³/s.

TABLE 2. METHODS USED TO STUDY THE MAGMATIC VARIATIONS
THROUGH TIME FOR THE DIFFERENT HOTSPOTS

	WAS	Bat/Grav	Mag. anomaly	Rad.	Lith. strength
Iceland	x		x	x	
Tristan		x		x	
St. Helena		x		x	
Cape Verde	x			x	
Canaries	x			x	
Madeira				x	
Azores	x		x	x	
Afar	x			x	
Hawaii	x	x	x	x	x
Louisville			x	x	
Pacific seamounts				x	x
Galápagos	x		x	x	
Samoa				x	
Ontong Java	x		x	x	
Tasmantid				x	
Easter			x	x	
La Réunion	x		x	x	
Kerguelen	x		x	x	
Yellowstone	x			x	
Europe	x			x	

Note: WAS— wide-angle seismic (e.g., White, 1993); Bat/Grav—bathymetry and gravity (e.g., Adam et al., 2007); Mag. anomaly—magnetic anomalies (e.g., Mjelde et al., 2008); Rad.—radiometric dating (e.g., Koppers et al., 2004); and Lith. strength—lithospheric strength (e.g., Hillier, 2007).
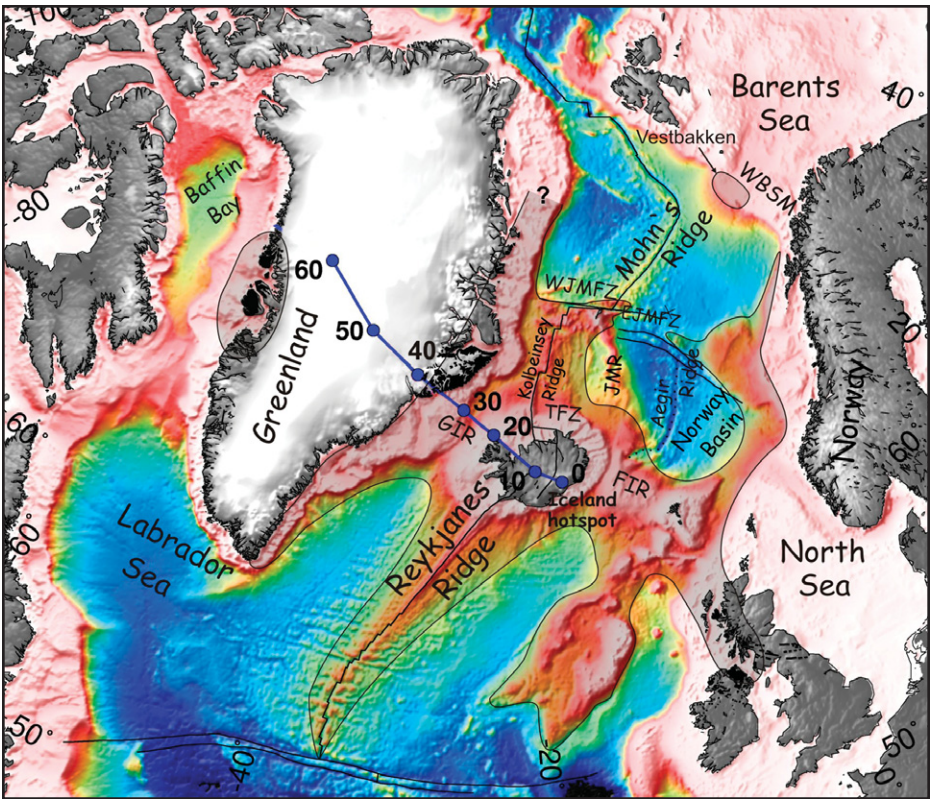

Figure 2. Location map of the Iceland hotspot in the North Atlantic. ETOPO-2 shaded relief bathymetry and topography are based on data from Sandwell and Smith (1997). Hotspot tracks are from Lawver and Müller (1994). Black areas onshore Greenland and the British Isles indicate early Tertiary basalt flows or dikes. The area influenced by the Iceland hotspot since ca. 70 Ma is shaded (from Mjelde et al., 2008). GIR—Greenland-Iceland Ridge; FIR—Faroe-Iceland Ridge; W/EJMFZ—west/east Jan Mayen fracture zone; WBSM—Western Barents Sea margin; JMR—Jan Mayen Ridge.

Tristan

The Tristan de Cunha hotspot generated the Walvis Ridge (Fig. 3), which can be traced back to continental separation off Namibia in the Early Cretaceous (126–137 Ma; Rabinowitz and LaBrecque, 1979; Elliott et al., 2009). The Walvis Ridge forms an up to 500-km-wide zone of seamounts and small ridges. This volcanic chain is generally considered to have been generated by a mantle plume interacting with the overlying African plate, and that the center of present-day activity is located near the island of Tristan da Cunha (O'Connor and Duncan, 1990).

Adam et al. (2007) presented an estimate of the variation of Qs and Qv along the Walvis Ridge since 65 Ma. They found peaks in Qs at 10 Ma, 38 Ma, and 54 Ma, and start of a long-period increase at 23 Ma. Their estimated peaks in Qv are 10 Ma, 39 Ma, and 59 Ma. The correlation between Qv and Qs suggests generation by a single mantle plume (Adam et al., 2007). These authors calculated the total volcanic volume for the ridge at 21.4×10^5 km^3 and the average volcanic flux as 1 m^3/s.

St. Helena

The St. Helena chain extends from the Josephine seamount (2.6 Ma) to a seamount dated to 81 Ma located near Cameroon (Fig. 3; O'Connor and Duncan, 1990). The northeastward extension of the chain, the Cameroon Line, does not express simple age progression (Adam et al., 2007). The St. Helena chain is characterized by a broad band of scattered seamounts and volcanic ridges with a similar age progression on the African plate as the Walvis Ridge. The origin of the St. Helena chain is associated with the emplacement of the Brazilian seamounts on the American plate (O'Connor and le Roex, 1992).

Adam et al. (2007) estimated the variation of Qs and Qv along the St. Helena chain since 50 Ma. They found a broad peak in Qs centered at 30 Ma. The width of the peak can be explained by the presence of two adjacent swells. Adam et al. (2007) found peaks in Qv at 10 Ma and 30 Ma. The lack of strong correlation between variations in Qv and Qs and the presence of two swells indicate that the St. Helena

trail is formed by two mantle plumes. Adam et al. (2007) estimated the total volcanic volume for the ridge at 11.1×10^5 km^3 and the average volcanic flux as 0.8 m^3/s.

Cape Verde

The Cape Verde Islands consist of nine islands located 500–800 km west of Africa (Fig. 4). The islands are situated in the southwestern part of the Cape Verde Rise, which is elevated 2–4 km above the underlying Jurassic-Cretaceous seafloor. The rise is considered to represent a hotspot swell (Crough, 1978).

The onset of the magmatism is estimated at ca. 21 Ma (Plesner et al., 2003; Lodge and Helffrich, 2006; Holm et al., 2008). A magmatic peak occurred at ca. 15 Ma (Holm et al., 2008), another at ca. 11 Ma (Plesner et al., 2003; Holm et al., 2008), and a later peak is centered at ca. 5 Ma (Holm et al., 2008). The total volume of magmatic rocks emplaced in the crust is estimated at 57×10^4 km^3 (Holm et al., 2008). This represents an average emplacement rate of 0.9 m^3/s.

Canaries

The Canary Province forms a 700-km-long and 400-km-wide distribution of volcanoes (Fig. 4). Volcanism on single islands can span over more than 20 m.y., generally consisting of a voluminous shield stage lasting 5–10 m.y. followed by a low-volume rejuvenation stage (Geldmacher et al., 2005). The spatial distribution and age variation of the volcanism are complex, but a crude age progression has been recognized (e.g., McDougall and Schmincke, 1976).

The Canary hotspot track appears to have started at ca. 68 Ma, an age obtained from a sample dredged from Lars Seamount (Geldmacher et al., 2001). These authors also report apparent magmatic pulses at ca. 55 Ma and 47 Ma. Another peak has been estimated at ca. 30 Ma (Stillman et al., 1975; Feraud et al., 1985; Geldmacher et al., 2005; Gutiérrez et al., 2006), and a long period of increased magmatism started around 23 Ma (Feraud et al., 1985; Schirnick et al., 1999; Geldmacher et al., 2001; Ancochea et al., 2006; Gutiérrez et al., 2006; Patriat and Labails, 2006; Carracedo et al., 2007; Meco et al., 2007; Camacho et al., 2009). A magmatic increase is reported at 15 Ma (Feraud et al., 1985; Hoernle and Schmincke, 1993; Ancochea et al., 2006; Gutiérrez et al., 2006; Meco et al., 2007; Menéndez et al., 2008), and a peak is centered at 10 Ma (Feraud et al., 1985; Schirnick et al., 1999; Geldmacher et al., 2005; Paris et al., 2005; Ancochea et al., 2006;
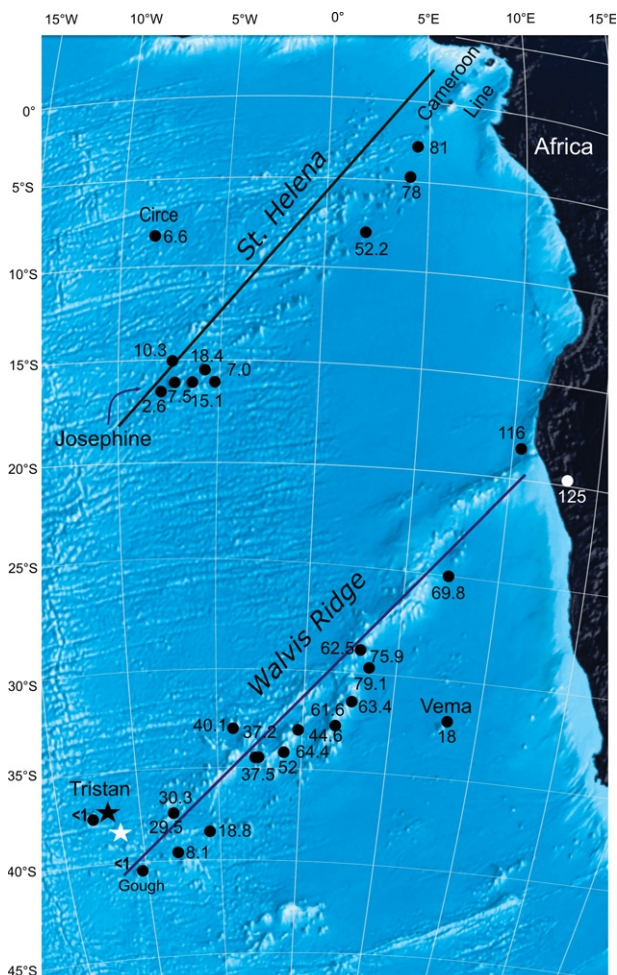

Figure 3. Seafloor topography along the St. Helena and Walvis chains (from Google Earth, bathymetry), and published volcanic ages (in Ma; from O'Connor and Duncan, 1990; O'Connor and le Roex, 1992). Black lines indicate the traces used to study the temporal evolution of hotspot fluxes (Adam et al., 2007). The white and black stars indicate the present-day location of the Walvis plume inferred by Courtillot et al. (2003) and Steinberger (2000), respectively.
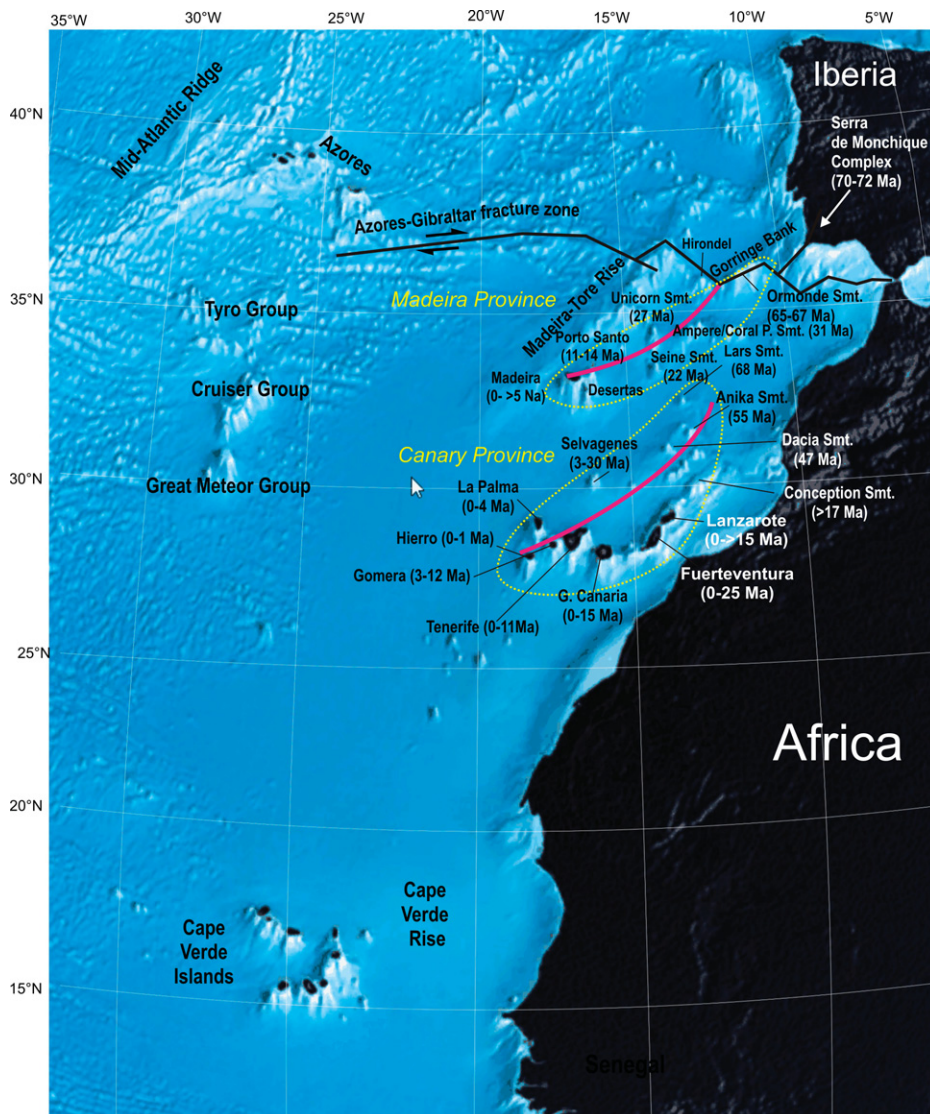
Figure 4. Location of the Cape Verde, Canary, Madeira, and Azores hotspots (seafloor topography from Google Earth, bathymetry). Hotspot tracks (in red) and ages for the Canary and Madeira hotspots are from Geldmacher et al. (2005, 2006).

Gutiérrez et al., 2006; Meco et al., 2007). A final magmatic peak is found around 5 Ma (Hoernle and Schmincke, 1993; Feraud et al., 1985; Paris et al., 2005; Ancochea et al., 2006; Longpré et al., 2008; Meco et al., 2007; Menéndez et al., 2008; Camacho et al., 2009; Patriat and Labails, 2006). A magmatic production rate of 0.7 m³/s was estimated for the Canary Islands by Schmincke and Sumita (1998).

Madeira

The Madeira Province consists of the Madeira hotspot track and the Madeira-Tore Rise (Fig. 4). The Madeira hotspot track forms a roughly 700-km-long and 200-km-wide chain of volcanoes with a rough southwest to north-

east progression of increasing ages (Fig. 4; Geldmacher et al., 2005). It can possibly be linked to the Serra de Monchique (70–72 Ma) igneous complex in southern Portugal (Geldmacher et al., 2005). The Madeira-Tore Rise is an ~1000-km-long submarine ridge located north of the Madeira hotspot track. The northern termination of the ridge is related to the active Azores Gibraltar fracture zone system (Africa-Eurasia plate boundary; e.g., Jiménez-Munt et al., 2001).

Pulses of increased magmatic activity forming seamounts have been dated to: ca. 66 Ma, 31 Ma, 27 Ma, and 22 Ma along the Madeira hotspot track (Geldmacher et al., 2006). Along the Madeira hotspot track and the Madeira-Tore Rise, additional pulses are centered at

roughly 12 Ma and 4 Ma (Geldmacher et al., 2001, 2006). The average emplacement rate of crustally emplaced magmatic rocks since 10 Ma was estimated by Geldmacher et al. (2001) to be 0.2 m³/s.

Azores

The Azores area is considered to reflect a typical ridge-hotspot interaction because of an anomalously elevated spreading ridge (e.g., Vogt, 1976), characteristic basalt geochemistry (e.g., Schilling, 1975), and gravity anomalies (e.g., Detrick et al., 1995; Fig. 4). The presence of a large region of elevated seafloor, associated with a thick crust between the Great Meteor Seamounts and the Azores platform, indicates that these hotspot-derived structures are genetically linked (Gente et al., 2003). We thus view them as part of the same magmatic system, dating back to ca. 85 Ma.

Dating of seamounts from the Cruiser Group suggests a pulse with increased magmatism at ca. 65 Ma, and several Great Meteor seamounts are clustered around roughly 42 Ma (Gente et al., 2003). Renewed melt supply around 20 Ma started the formation of the Azores Plateau (Gente et al., 2003). A later magmatic pulse appears to be centered around 9 Ma (Cannat et al., 1999). From the estimates of excess crustal thickness presented by Cannat et al. (1999), we calculate the average emplacement rate since 10 Ma as 0.7 m³/s.

Afar

The East African, Red Sea, and Gulf of Aden rifts are strongly associated with magmatism related to the Afar plume (Fig. 5; e.g., Courtillot et al., 1999; Chorowicz, 2005). The onset of the magmatism occurred in the Lake Turkana region, Kenya, around 45 Ma (Hofmann et al., 1997; George et al., 1998; Rogers et al., 2000; Furman et al., 2006; Bastow et al., 2008; Corti, 2009), and a magmatic pulse is reported at 40 Ma (Courtillot et al., 1999; Coulié et al., 2003; Chorowicz, 2005; Bastow et al., 2008; Beccaluva et al., 2009; Corti, 2009). Increased magmatism related to the main Afar plume is reported to have started at 30 Ma (White, 1993; Hofmann et al., 1997; Orihashi et al., 1998; Courtillot et al., 1999; Coulié et al., 2003; Kieffer et al., 2004; Chorowicz, 2005; Park et al., 2007; Meshesha and Shinjo, 2008; Bastow et al., 2008; Beccaluva et al., 2009; Corti, 2009; Krienitz et al., 2009). Another important increase in magmatism is reported to have started at ca. 23 Ma (White, 1993; Courtillot et al., 1999; Renne et al., 1999; Coulié et al., 2003; Kieffer et al., 2004;
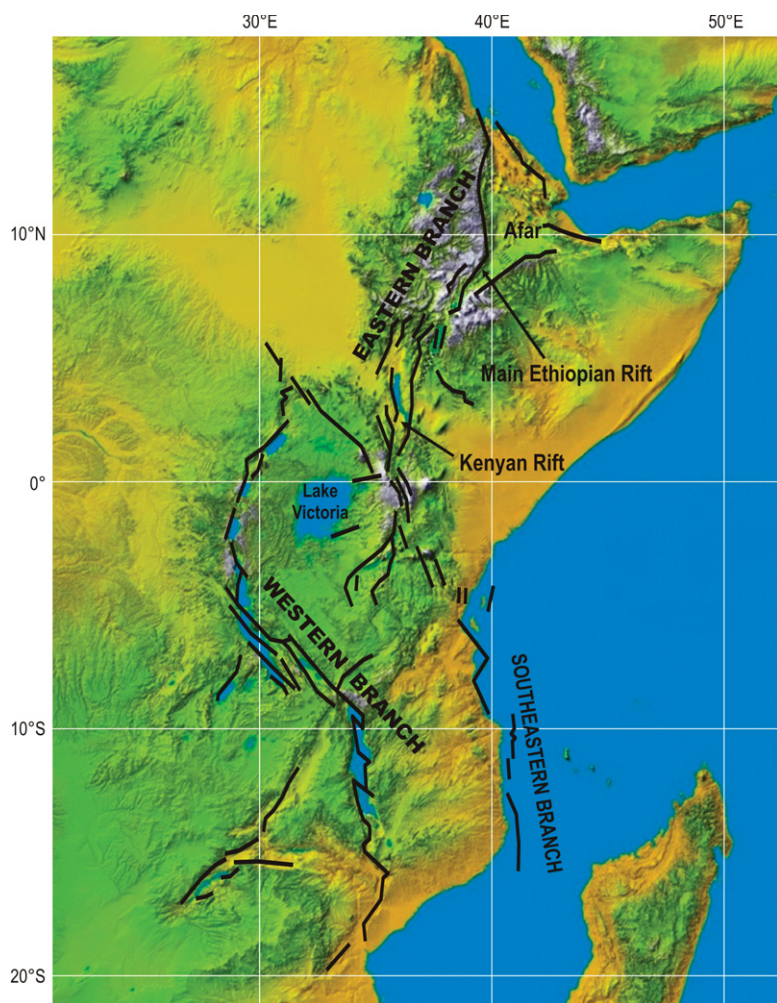
Figure 5. Location of the Afar–East African tectono-magmatic province. Geographical map is based on National Aeronautics and Space Administration (NASA) radar topography image, and main geological features are from Chorowicz (2005). Black lines—faults.

Van Ark and Lin, 2004). The average Cenozoic magmatic emplacement rate has been estimated at 2.5 m³/s prior to 22 Ma, increasing to 6 m³/s thereafter (Vidal and Bonneville, 2004; Van Ark and Lin, 2004).

Louisville

The Louisville seamount track is a 4300-km-long chain of submarine volcanoes located in the South Pacific, which is inferred to have been generated by a mantle plume since around 80 Ma (Fig. 6; Lonsdale, 1988). The Hollister Ridge is a 450 km linear chain of seamounts to some extent genetically related to the Louisville hotspot (Wessel and Kroenke, 1997; Vlastélic and Dosso, 2005). Pulses with increased magmatic activity appear at ca. 67 Ma (Lonsdale, 1988), 60 Ma (Lonsdale, 1988; Koppers et al., 2004), 56 Ma, 48 Ma, 41 Ma, 25 Ma, 20 Ma (Lonsdale, 1988), 12 Ma (Lonsdale, 1988; Koppers et al., 2004), and 3 Ma (Hollister Ridge; Vlastélic et al., 1998). The average magmatic production for the Louisville plume was estimated by Lonsdale (1988) as 0.1 m³/s prior to ca. 15 Ma, decreasing by an order of magnitude to 0.01 m³/s thereafter.

Pacific Seamounts

Hillier (2007) estimated the eruption ages of 2700 Pacific volcanoes. The study included seamounts related to the following chains: Hawaii, Louisville, Society, Easter Island, Cook/Austral, Foundation, Puka-Puka, Pitcairn, Marquesas, Guadalupe, Cobb, and Bowie (Figs. 6 and 7). The Early Cenozoic eruption rate was estimated at 1.6 m³/s, increasing to 2.9 m³/s at ca. 50 Ma, and 3.9 m³/s at ca. 30 Ma. The average Cenozoic eruption rate is measured at 2.2 m³/s.

Galápagos

The Galápagos hotspot has formed volcanic tracks on the Cocos and Nazca plates, extending from the Galápagos Islands to the Central American and Ecuadorian trenches (Fig. 7). The hotspot track off the coast of Costa Rica consists of the Cocos Ridge (e.g., Werner et al., 1999). On the Nazca plate, the Coiba Ridge, Malpelo Ridge, Carnegie Ridge, and Galápagos Plateau are associated with the hotspot (e.g., Lonsdale and Klitgord, 1978). Hoernle et al. (2002) argued that up to 71-m.y.-old igneous complexes along the Pacific margin of Costa Rica and Panama represent the accreted history of the Galápagos hotspot, linking the hotspot to the Caribbean large igneous province (ca. 72–95 Ma). These authors related larger accretion rates to higher magma production rates, and identified the start of a magmatic pulse at ca. 65 Ma.

Chorowicz, 2005; Park et al., 2007; Meshesha and Shinjo, 2008; Bastow et al., 2008; Beccaluva et al., 2009; Corti, 2009; Krienitz et al., 2009). In this pulse, we have incorporated a magmatic event starting at 19 Ma cited by several authors (e.g., George et al., 1998). A later magmatic pulse is centered around 10 Ma (Courtillot et al., 1999; Coulié et al., 2003; Kieffer et al., 2004; Chorowicz, 2005; Park et al., 2007; Meshesha and Shinjo, 2008; Bastow et al., 2008; Beccaluva et al., 2009; Corti, 2009; Krienitz et al., 2009), and a final one is reported at ca. 4 Ma (White, 1993; Chorowicz, 2005; Meshesha and Shinjo, 2008; Corti, 2009; Krienitz et al., 2009). George et al. (1998) estimated the magmatic emplacement rate during the arrival of the main plume pulse (30–28 Ma) at 4.8 m³/s, and they calculated an average rate of 1.6 m³/s for the past 30 m.y.

Hawaii

The Hawaii-Emperor hotspot has the longest and clearest hotspot track on Earth (0–80 Ma) and is generally associated with a mantle plume originating from the core-mantle boundary (Fig. 6; e.g., Courtillot et al., 2003; Van Ark and Lin, 2004). Magmatic pulses along the track have been estimated at around 64 Ma (Van Ark and Lin, 2004), ca. 50 Ma (White, 1993; Vidal and Bonneville, 2004; Van Ark and Lin, 2004), ca. 42 Ma (Vidal and Bonneville, 2004; Van Ark and Lin, 2004), and at ca. 28 Ma (Van Ark and Lin, 2004). A general increase in magmatism occurred around 22 Ma (White, 1993; Vidal and Bonneville, 2004; Van Ark and Lin, 2004), and later pulses were centered at 14 Ma (White, 1993; Vidal and Bonneville, 2004) and 3 Ma (White, 1993; Vidal and Bonneville, 2004;
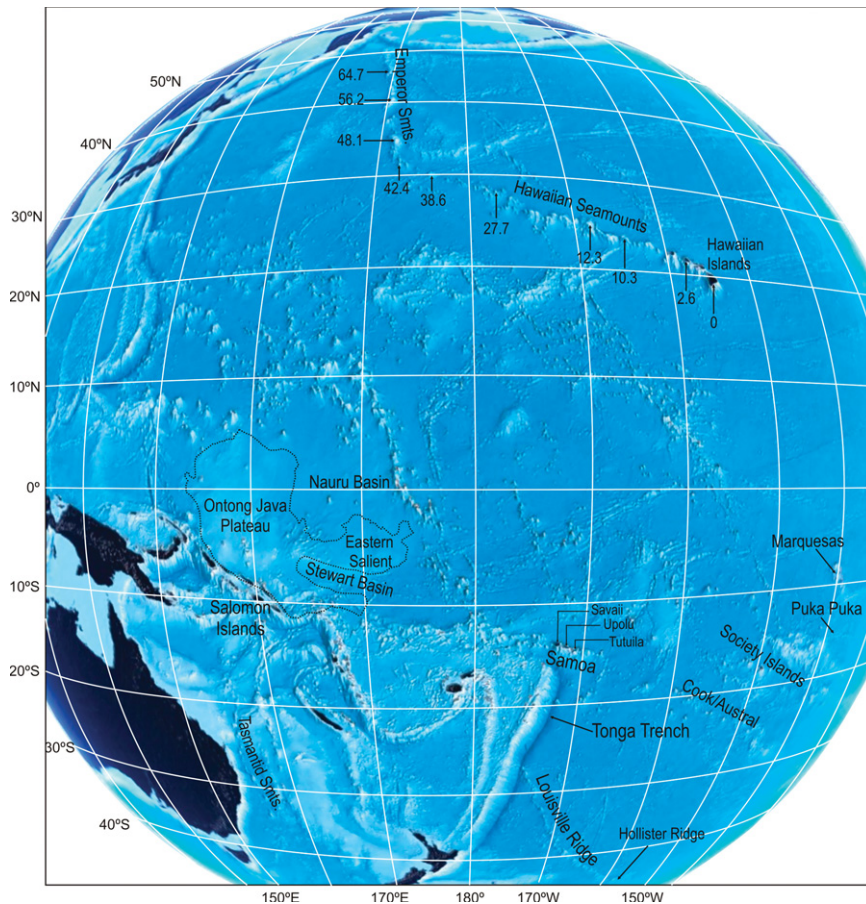
Figure 6. Location of the Hawaiian, Samoan, Louisville, and Tasmantid hotspots, as well as the Ontong Java Plateau and other Pacific seamounts (seafloor topography from Google Earth, bathymetry). Ages in Ma for the Hawaiian and Emperor chains are from Vidal and Bonneville (2004).
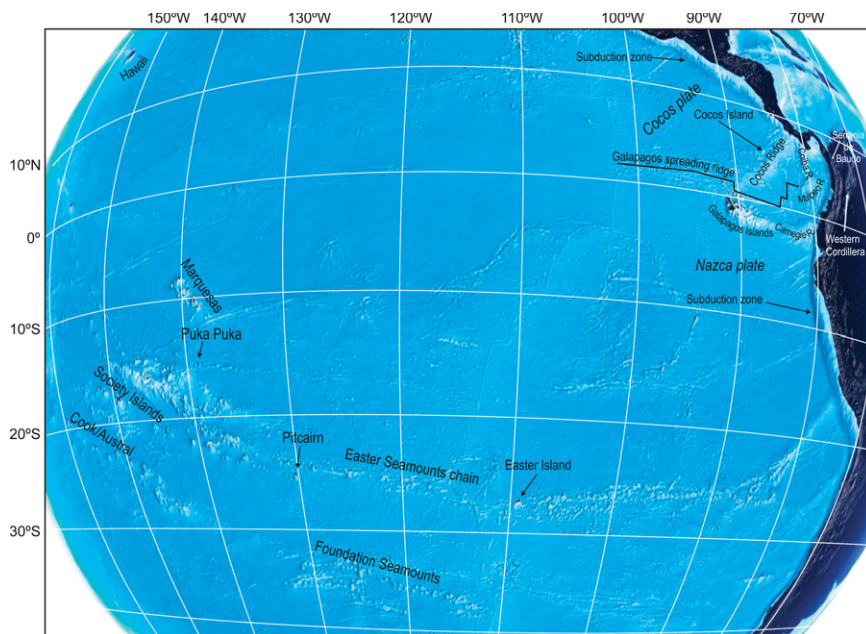

Figure 7. Location of the Galápagos and Easter hotspots, as well as other Pacific seamounts (seafloor topography from Google Earth, bathymetry).

The same event has been noted by Geldmacher et al. (2003). Hoernle et al. (2002) estimated magmatic pulses centered at ca. 39 Ma and 33 Ma, and longer pulses starting around 21 Ma and 9 Ma. Geldmacher et al. (2003) discussed a Miocene pulse centered at 14 Ma. Based on measurements of crustal thickness of the ridges associated with the Galápagos hotspot (Detrick et al., 2002; Sallarès et al., 2003; Marcaillou et al., 2006), we estimate the magmatic production rate since 20 Ma at 5 m^3/s.

Samoa and Society

The Samoan Islands and seamounts form a westward age-progressing hotspot track from the present-day hotspot location of Vailulu'u (Fig. 6; Hart et al., 2004; Koppers et al., 2008). Seismic tomography indicates that the Samoan plume stem extends into the lower mantle (Montelli et al., 2004), and it presently interacts dynamically with the Tonga slab (e.g., Hawkins and Natland, 1975). Hart et al. (2004) dated the start of the Samoan magmatism at ca. 23 Ma, and these authors described another peak in magmatism at ca. 11 Ma. A final peak is centered around 3 Ma (Hart et al., 2004; Koppers et al., 2008). Based on mantle upwelling rates described by Sims et al. (2008), we estimate the Samoan magmatic production rate at 2 m^3/s. The islands and atolls of the Society archipelago form an 800-km-long volcanic lineament appearing at roughly 4 Ma (Fig. 6; Duncan and McDougall, 1976; Clouard and Bonneville, 2001; Guillou et al., 2005; Uto et al., 2007).

Ontong Java and Tasmantid

The Ontong Java Plateau is Earth's most voluminous large igneous province, dominantly emplaced in Early Cretaceous at 122 Ma (Fig. 6; Coffin and Eldholm, 1994). The plateau has experienced a complex history and includes terrains associated with a mantle plume, normal oceanic crust, and arc magmatism (Petterson et al., 1999; Fitton et al., 2004). Petterson et al. (1999) reported Cenozoic episodes of increased magmatism centered at roughly 63 Ma, 34 Ma, and longer episodes starting around 44 Ma, 24 Ma, and 8 Ma. Based on the Cenozoic magmatic production rate of 3 m^3/s estimated for the Kerguelen Plateau (Coffin et al., 2002), and the calculations indicating that the production rate for Ontong Java was three times higher during Cretaceous (Coffin and Eldholm,1994), we infer a Cenozoic production rate for Ontong Java of 9 m^3/s. The collision between the Ontong Java Plateau and the Australian plate is documented in a bend in the Tasmantid hotspot at 26–23 Ma

(Fig. 6). For this hotspot, magmatic peaks are centered at around 24 Ma, 21 Ma, 16 Ma, and 7 Ma (Knesel et al., 2008).

Easter

The Easter Seamount Chain is an ~3000-km-long zone of islands, seamounts, and anomalously high topography extending from near the East Pacific Rise in the west to the southern tip of the Nazca Ridge (Fig. 7). Although other models have been proposed, the ridge is generally considered to represent a hotspot track (e.g., Morgan, 1971; Cheng et al., 1999). The first magmatism along the chain is reported at roughly 30 Ma (Cheng et al., 1999), and later magmatic peaks appear around 26 Ma (Haase et al., 2000), ca. 22 Ma (O'Connor et al., 1995; Cheng et al., 1999; Haase et al., 2000), 15 Ma (O'Connor et al., 1995), 8 Ma (O'Connor et al., 1995; Cheng et al., 1999), and 3 Ma (O'Connor et al., 1995; Cheng et al., 1999). To our knowledge, available estimates of volumetric production are insufficient to calculate the production rate through time.

La Réunion

The Chagos and Mascarene Plateaus, as well as the Mauritius and La Réunion islands in the Indian Ocean (Fig. 8), are regarded as volcanic constructions of a hotspot that can be traced back to the emplacement of the Deccan Traps at ca. 65 Ma (Duncan et al., 1989; White, 1993; Bonneville et al., 1997; Todal and Edholm, 1998; Luais, 2004). Later magmatic peaks appear around 57 Ma (Todal and Edholm, 1998; Paul et al., 2005), 48 Ma (Paul et al., 2005), 35 Ma (Duncan et al., 1989; Bonneville et al., 1997; Paul et al., 2005), 8 Ma (Bonneville et al., 1997; Charvis et al., 1999; Paul et al., 2005), and 2 Ma (Bonneville et al., 1997; Luais, 2004; Paul et al., 2005; Michon et al., 2007). The magmatic production rate was calculated by White (1993) at 160 m^3/s during the emplacement of the Deccan Traps, decreasing to an average value of 1.3 m^3/s since 20 Ma.

Kerguelen

The Kerguelen hotspot has caused magmatism in the eastern Indian Ocean region since around 130 Ma (Fig. 8; e.g., Duncan, 1978). The igneous rock complexes have been widely dispersed due to changing motions of the Indian, Australian, and Antarctic plates (Müller et al., 1993). The Kerguelen large igneous province includes, in decreasing age order, Bunbury (Australia), Rajmahal (India), dikes on the conjugate Indian/Antarctica margins, Southern Kerguelen Plateau, Elan Bank, Central Kerguelen Plateau,
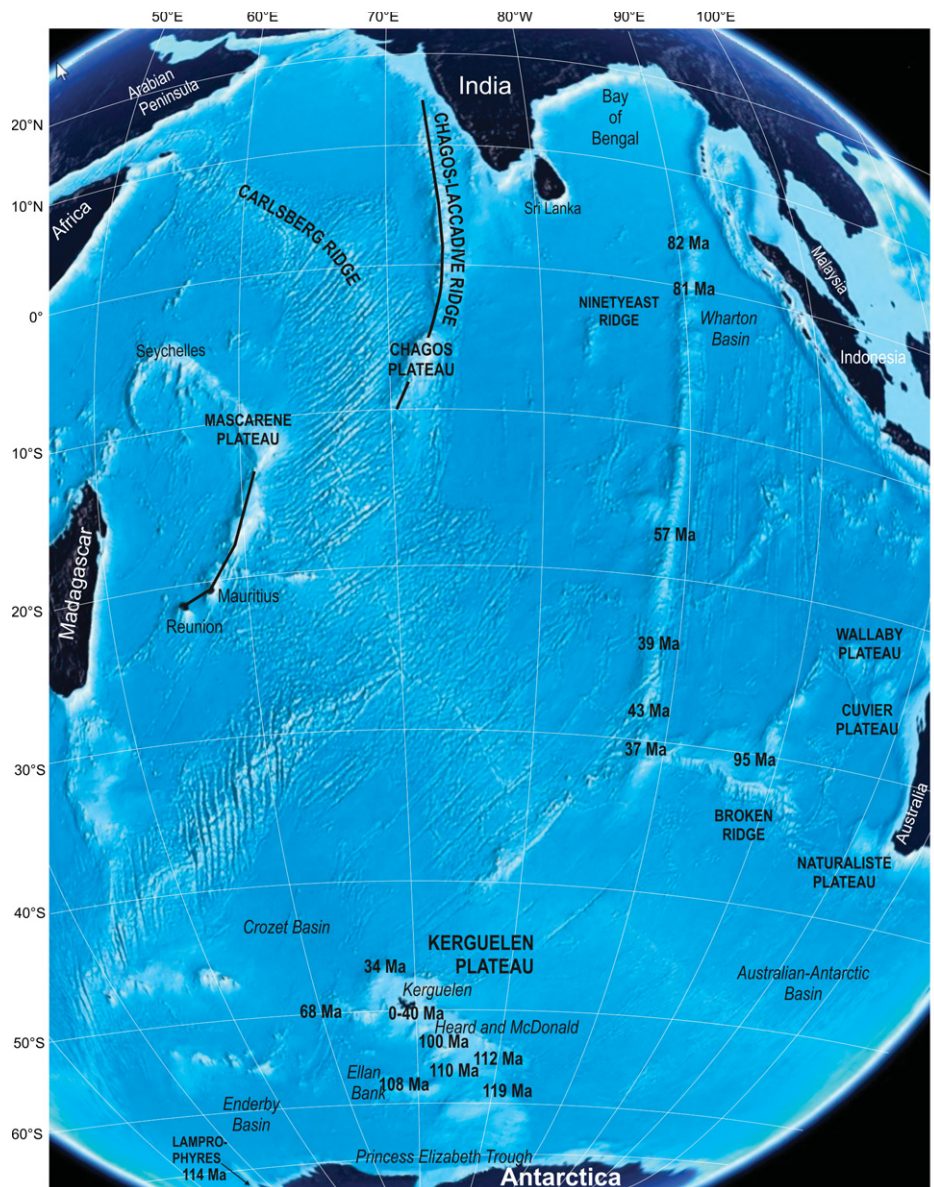
Figure 8. Location of the Kerguelen and Réunion hotspots (seafloor topography from Google Earth, bathymetry). Ages for the Kerguelen hotspot are from Coffin et al. (2002), and the Réunion hotspot track is from Duncan and Storey (1992).

Broken Ridge, Ninetyeast Ridge, Skiff Bank, Northern Kerguelen Plateau, and Kerguelen Archipelago, as well as Heard and McDonald Islands (Coffin et al., 2002). The start of a long period of increased magmatism along the Ninetyeast Ridge at roughly 60 Ma was reported by Verzhbitsky (2003), and the start of another period has been dated at ca. 40 Ma (Nicolaysen et al., 2000; Coffin et al., 2002; Doucet et al., 2005). A magmatic pulse appears to be centered at 34 Ma (Weis et al., 2002; Ingle et al., 2003; Doucet et al., 2005), and 30 Ma marked the start of a long period with increased activity (Nicolaysen et al., 2000; Coffin et al., 2002; Wallace

et al., 2002; Weis et al., 2002; Ingle et al., 2003; Doucet et al., 2005; Xu et al., 2007). Later pulses are centered around 20 Ma (Coffin et al., 2002; Weis et al., 2002), 9 Ma (Weis et al., 2002; Ingle et al., 2003), and 2 Ma (Weis et al., 2002). The average Cenozoic magmatic production rate has been estimated to be 3 m^3/s (Coffin et al., 2002).

Yellowstone

The Yellowstone hotspot track extends 800 km across the northern Basin and Range Province, United States (Fig. 9). The youngest manifestation of the hotspot is associated
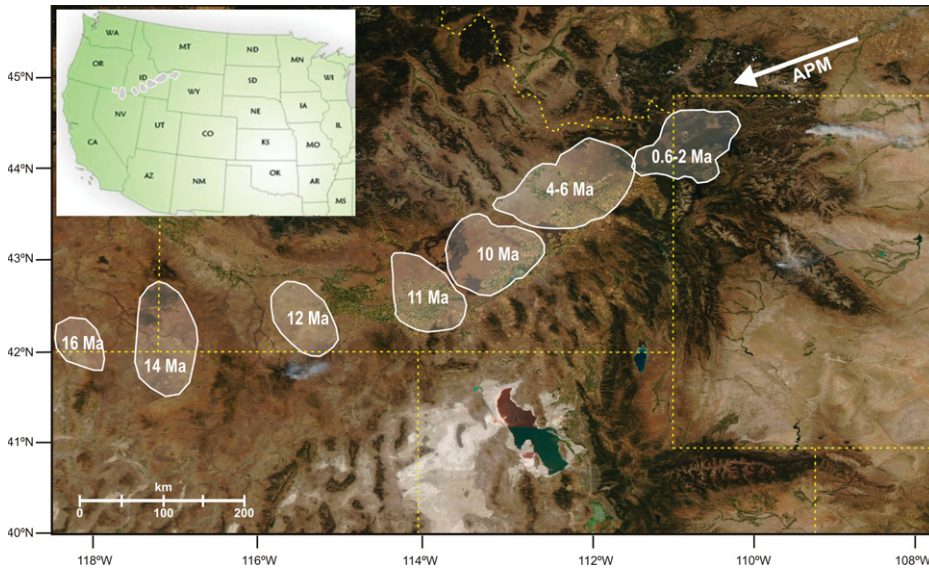
Figure 9. Location of the Yellowstone hotspot. Geographical map is based on National Aeronautics and Space Administration (NASA) *Aqua* satellite data. Approximate ages of silicic volcanic centers are noted in Ma (from Waite et al., 2006). The white lines outline the locations of the eruptive centers. State boundaries in the western United States are plotted for reference. The direction of absolute plate motion (APM) from Gripp and Gordon (2002) is shown with a white arrow.

has revealed a range of upper-mantle anomalies (e.g., Ritter et al., 2001), but the magmatism is not consistent with a time-regressive hotspot track. To our knowledge, available estimates of the magmatic production of the region are insufficient to calculate the production rate through time.

Cenozoic Magmatic Peaks

Table 4 indicates that the pattern of investigated magmatism is not randomly distributed with time. Primary peaks may be identified at 10 Ma, 22 Ma, 30 Ma, 40 Ma, 49 Ma, and 60 Ma, and secondary peaks at 4 Ma, 15 Ma, 34 Ma, 45 Ma, and 65 Ma. Spectral analysis using Burg's method (well suited for short time series) seems to confirm a dominant period of ~10 m.y. (10 Ma, 20 Ma, etc.), and a secondary period of ~5 m.y. (5 Ma, 15 Ma, etc.; Fig. 11), but we cannot be sure because the limited data set at our disposal prevents us from obtaining meaningful confidence levels. The observations may be filtered by assuming that one measurement has been erroneously located in time for each million years. By removing one measurement from each million-year period in Table 4 (unfiltered), the inferred pattern becomes clearer (Table 4, filtered). The spectrum also hints at a possible ~15 m.y. period, as has been reported for Hawaii and Iceland (Van Ark and Lin, 2004; Mjelde and Faleide, 2009).

with extensive geysers and hot springs in Yellowstone National Park. Yellowstone's mantle source has often been attributed to a mantle plume (e.g., Morgan, 1972), and an upper-mantle low-velocity anomaly has been mapped by teleseismic tomography (Waite et al., 2006). The start of the magmatism has been estimated to be around 18 Ma (Schutt et al., 2008), and magmatic peaks appear around 11 Ma and 5 Ma (Waite et al., 2006; Stachnik et al., 2008). Based on the value of mantle buoyancy flux given by Schutt et al. (2008), we estimate the magmatic production rate at 0.2 m³/s.

Europe

Widespread anorogenic magmatism, unrelated to subduction-zone modification of the mantle source, developed within the Mediterranean and surrounding regions during the Cenozoic (Fig. 10). The magmatism is generally referred to as the Circum-Mediterranean anorogenic Cenozoic igneous province. Lustrino and Wilson (2007) presented a thorough review of the spatial evolution of the magmatism through the Cenozoic. Their observations for different European regions are outlined in Table 3, and a summary of the entire province is included in Table 4. We have treated the Canary and Madeira hotspot as separate provinces. Magmatic peaks may be found around 60 Ma (Italy, Germany, Carpathians, Libya), 45 Ma (Morocco, Germany), 41 Ma (Germany, Libya, Mashrek), 21 Ma (Spain, Germany, Bohemian Massif), 15 Ma (Germany, Carpathians), 10 Ma (entire region except Germany and Bohemian Massif), and 3 Ma (Spain, Italy, Carpathians, Macedonia). Global tomography
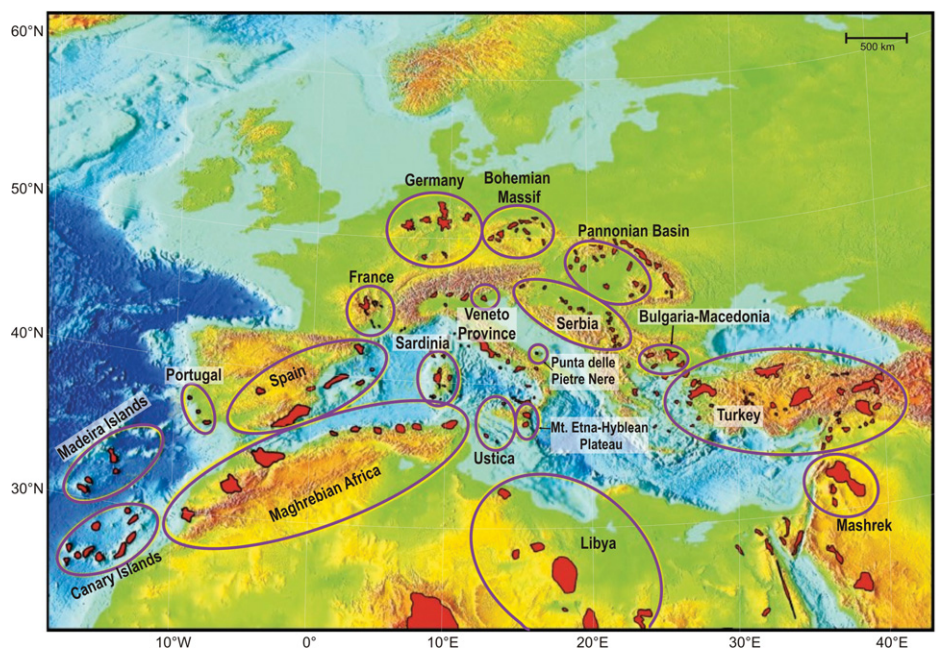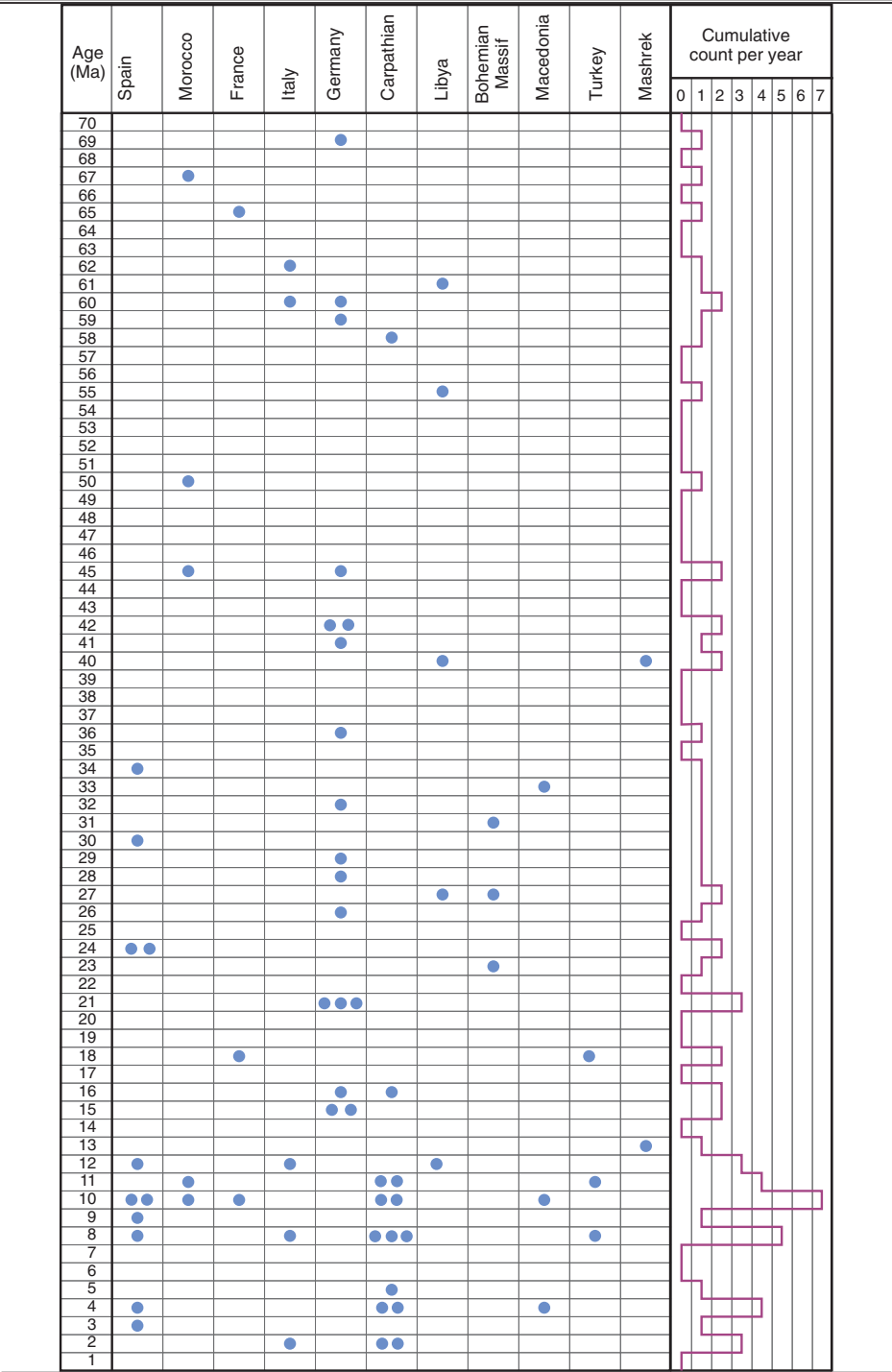

Figure 10. Topography of the circum-Mediterranean area showing the locations of Cenozoic igneous provinces (modified from Lustrino and Wilson, 2007). The circled areas refer to anorogenic provinces discussed in this paper.

TABLE 3. VARIATION OF ANOROGENIC MAGMATISM WITHIN THE MEDITERRANEAN AND SURROUNDING REGIONS DURING THE CENOZOIC

Age (Ma)	Spain	Morocco	France	Italy	Germany	Carpathian	Libya	Bohemian Massif	Macedonia	Turkey	Mashrek	Cumulative count per year
70												
69					•							
68												
67		•										
66												
65			•									
64												
63												
62				•								
61							•					
60				•	•							
59						•						
58							•					
57												
56												
55							•					
54												
53												
52												
51												
50		•										
49												
48												
47												
46												
45		•			•							
44												
43												
42						• •						
41					•							
40							•				•	
39												
38												
37												
36					•							
35												
34	•											
33									•			
32					•							
31								•				
30	•											
29					•							
28					•							
27							•	•				
26					•							
25												
24	• •											
23								•				
22												
21						• • •						
20												
19												
18			•							•		
17												
16					•	•						
15					• •							
14												
13											•	
12	•			•			•					
11		•				• •				•		
10	• •	•	•			• •			•			
9	•											
8	•			•		• • •				•		
7												
6												
5						•						
4		•				• •			•			
3	•											
2				•		• •						
1												

Note: Table is based on Lustrino and Wilson (2007). Pulses of magmatism are indicated with blue circles, and the cumulative count per m.y. for the entire area is shown in the right column.

Magmatic Production Rates

Table 5 shows the magmatic production rate in m^3/s since ca. 20 Ma for the studied hotspots, sorted by hotspot rate. Nine hotspots have production >1 m^3/s, and eight have production <1 m^3/s. The production varies strongly within the group with high production, from 1.3 m^3/s (La Réunion), increasing by an average of 1.1 m^3/s per hotspot to 9 m^3/s (Ontong Java). The variation is smaller within the group with low production, from 0.2 m^3/s (Yellowstone), increasing by an average of 0.1 m^3/s per hotspot to 1 m^3/s (Tristan). The exception is Louisville, the production rate of which is one order of magnitude smaller than that of Yellowstone. The total production rate for all studied hotspots is estimated at 42.6 m^3/s, which is one order of magnitude smaller than the global production rate at oceanic spreading ridges (e.g., Cogné and Humler, 2006).
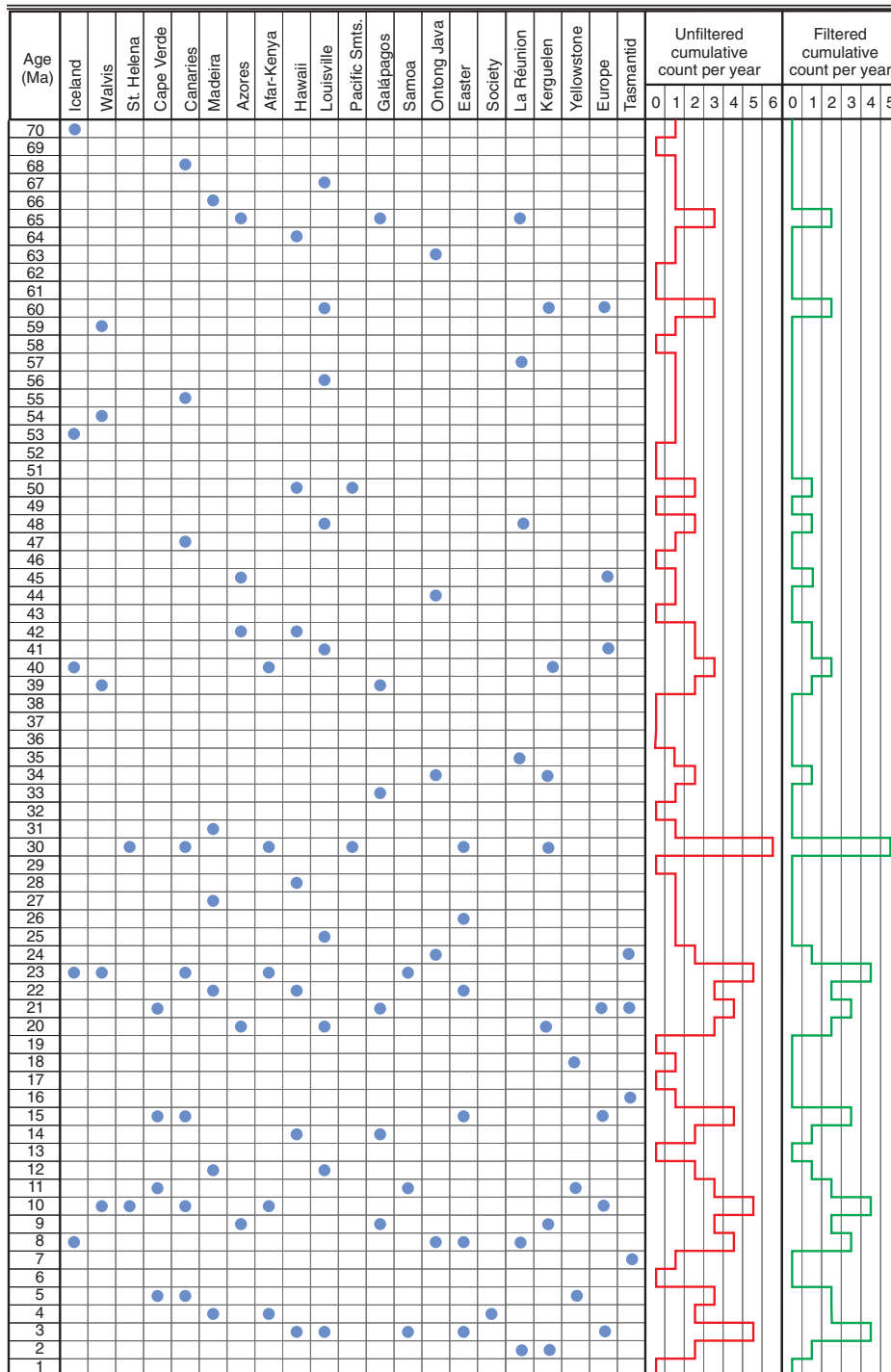
DISCUSSION: POSSIBLE CAUSES FOR THE INFERRED VARIATIONS IN MAGMATISM

Oceanic Spreading and Plate-Tectonic Reorganizations

Estimates of the rate of generation of oceanic crust at spreading ridges show large variability; Cogné and Humler (2006) calculated an ~50% increase in the production rate through the Cenozoic, whereas Becker et al. (2009) and Seton et al. (2009) found a similar decrease in the same period. Regardless, these trends do not seem to have the variability needed to explain the periodicities we have documented here.

Plate reorganizations are believed to impact the horizontal stresses in plates, and these stresses have been shown to modulate the permeability of the lithosphere to volcanism (e.g., Hieronymus and Bercovici, 2001). However, we are unaware of a global study of such effects, and, furthermore, it seems likely that these effects would be strongest near the primary cause of the reorganization (e.g., a collision or a new subduction zone). A global plate-tectonic reorganization occurred around 50 Ma, documented, for instance, by the Hawaiian-Emperor bend (e.g., Wessel and Kroenke, 2008). Another major plate-tectonic reorganization occurring at 26 Ma was most likely triggered by the collision of the Ontong Java Plateau with the Melanesian arc (Knesel et al., 2008). This event is recorded in the motion of the Australian plate, and it correlates well with offsets in hotspot seamount tracks on the Pacific plate, e.g., the Hawaiian chain (Kroenke et al., 2004). To our knowledge, no other global Cenozoic plate reorganizations

TABLE 4. VARIATION OF CENOZOIC MAGMATISM RELATED TO THE HOTSPOTS STUDIED

Age (Ma)	Iceland	Walvis	St. Helena	Cape Verde	Canaries	Madeira	Azores	Afar-Kenya	Hawaii	Louisville	Pacific Smts.	Galápagos	Samoa	Ontong Java	Easter	Society	La Réunion	Kerguelen	Yellowstone	Europe	Tasmantid	Unfiltered cumulative count per year	Filtered cumulative count per year
70	●																						
69																							
68				●																			
67									●														
66						●																	
65				●								●					●						
64							●																
63														●									
62																							
61																							
60									●									●		●			
59		●																					
58																							
57																	●						
56									●														
55					●																		
54		●																					
53	●																						
52																							
51																							
50							●			●													
49																							
48									●								●						
47					●																		
46																							
45												●								●			
44														●									
43																							
42								●	●			●											
41									●											●			
40	●						●											●					
39		●										●											
38																							
37																							
36																							
35																	●						
34														●				●					
33												●											
32																							
31					●																		
30		●		●	●					●					●								
29																							
28							●																
27					●																		
26															●								
25									●														
24														●							●		
23	●	●			●				●				●										
22					●	●									●								
21				●														●		●			
20						●			●								●						
19																							
18																		●					
17																							
16																					●		
15				●											●					●			
14							●					●											
13																							
12				●																			
11													●						●				
10		●	●	●			●													●			
9												●											
8	●														●	●							
7																					●		
6																							
5				●	●													●					
4						●	●									●							
3									●					●				●					
2																	●	●					
1																							

Note: Pulses of magmatism are indicated with blue circles. The European magmatism (Table 3) has been averaged to one column. The red column shows the (unfiltered) cumulative count per m.y. for all hotspots, whereas the green column shows the filtered version, where one count has been subtracted for each m.y.

have been reported. It should be noted that the only major plate-tectonic change occurring in the North Atlantic, at around 33 Ma (e.g., Eldholm et al., 1989), apparently did not modify the Icelandic hotspot production. It thus appears that the global variations in magmatism inferred in our study cannot be explained only by variations in oceanic accretion or plate-tectonic reorganizations. However, a stronger link between hotspot activity and global plate reorganizations has been inferred for the Cretaceous (e.g., Anderson, 1994), and we thus recognize that this issue merits further research.

Lithosphere Thickness

Magmatism resulting from mantle plumes is strongly controlled by the thickness of the overlying lithosphere (White, 1993). Thick lithosphere will hamper decompression melting, whereas thin lithosphere will lead to large quantities of melt produced by mantle decompression. Enhanced magmatism is hence found beneath young oceanic lithosphere, or beneath rifting lithosphere. It is possible that these factors may explain the inferred variations in magma production for the various hotspots studied. For example, the anomalous magmatism around breakup (ca. 53 Ma) for the Icelandic hotspot may be explained by increased decompression melting along the axis of rifting, and the magmatic pulse around 40 Ma may be related to increased decompression melting and small-scale convection when the plume was located near the Greenland shelf edge (e.g., Torsvik and Cocks, 2005). Another example concerns the Hawaiian ridge, where the variations in volcanic production appear to correlate with the various Pacific fracture zones (Van Ark and Lin, 2004). The Ninetyeast Ridge, constructed by the Kerguelen hotspot, represents a third oceanic example. The ridge forms a hotspot track from Late Cretaceous to around 35 Ma, and Coffin et al. (2002) related its cessation to emplacement on progressively older oceanic crust.

Although magmatism occurred earlier than the start of rifting in East Africa, the rifting process did to some extent control the variations in magmatism there (Chorowicz, 2005). Differences in lithospheric thickness have also played an important role during the emplacement of the products of widespread European magmatism (Lustrino and Wilson, 2007).

Plume-Ridge Interaction

Direct mantle plume–oceanic spreading ridge interaction may be invoked to explain the increased Iceland plume magmatism at ca. 23 Ma (Torsvik and Cocks 2005). In order
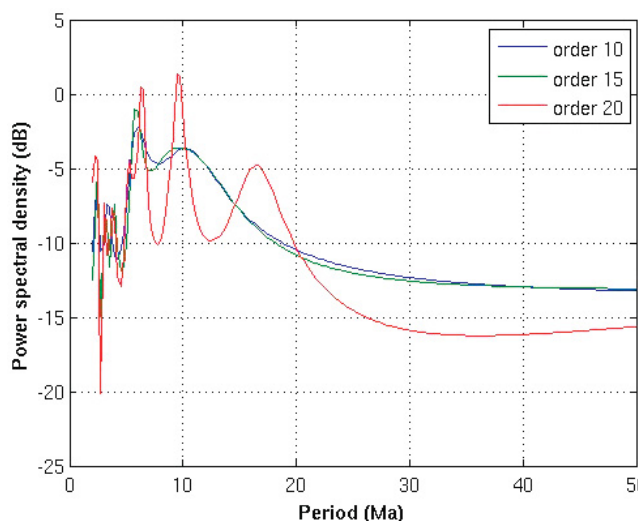
Figure 11. Power spectrum for the global magmatic flux since 70 Ma (based on Table 4, filtered cumulative count per year). The power density spectrum was estimated using the Burg parametric spectral estimation algorithm from the Matlab Signal Processing Toolbox. The Burg algorithm estimates the spectral content by fitting an autoregressive (AR) linear prediction filter model of a given order to the signal. The highest order used in our case was 20. Any linear trend (including the average) was removed from the data before spectral estimation. We also show results for two lower-order models, noting that the ~5 m.y. and ~10 m.y. trends appear to be robust features in all three estimates, whereas the ~15 m.y. peak only appears when we push the order toward the higher end.

TABLE 5. THE MAGMATIC PRODUCTION RATE SINCE CA. 20 Ma FOR THE STUDIED HOTSPOTS, SORTED BY PRODUCTION RATE
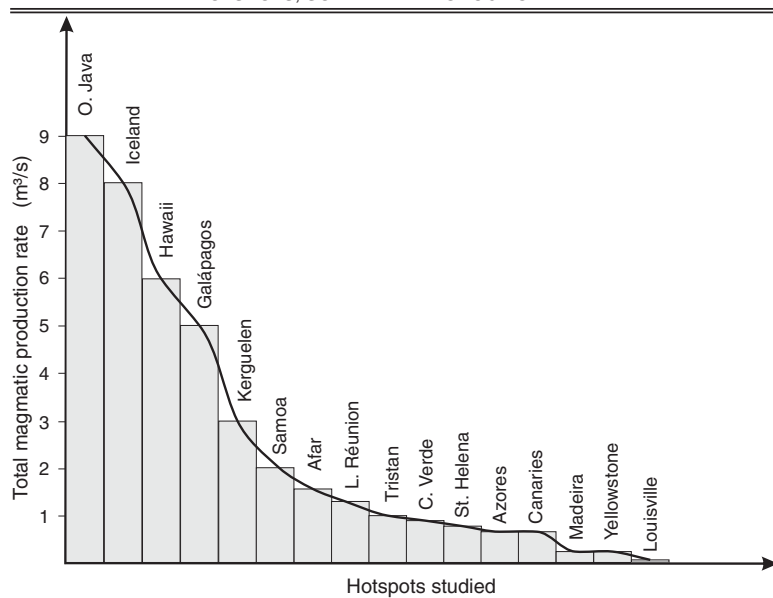
to explain the late Miocene pulse, Breivik et al. (2008) suggested a plume–spreading ridge interaction model related to asthenospheric flow away from Iceland. Strong interaction with spreading ridges has also occurred for the Azores, Galápagos, and Easter hotspots (e.g., Vogt, 1976; O'Connor et al., 1995; Geldmacher et al., 2003), and weaker interaction may be inferred for parts of the remaining oceanic hotspots studied.

Lower Mantle and Core

From these discussions, we can conclude that the observed variations in magmatic productivity can be explained by differences in lithospheric thickness and/or interaction with spreading ridges, when the hotspots are studied individually. It is, however, unlikely that such lithospheric–upper mantle processes can cause the inferred 5 and 10 m.y. global co-pulsations.

The 5–10 m.y. period of magmatic variations is within the range of estimates of the age contrasts between adjacent V-shaped ridges related to the Icelandic hotspot (Vogt, 1971; White et al., 1995). The ridges may be due to rift propagation (Hey et al., 2010), but they have also been modeled as resulting from pulsations in a mantle plume conduit (Ito, 2001). Such stable solitary waves may form in response to disturbances introduced into fully developed conduits (Olson and Christensen, 1986). Similar periodicities may be induced by plume separation effects at the 670 km discontinuity (Bercovici and Mahoney, 1994). Although such effects modulating the rising plume may successfully explain the pulsations observed for individual plumes, they fail to explain the observed co-pulsations.

The same applies to models involving plumes originating from a presumed thermochemical boundary layer at the base of the mantle (Lin and Keken, 2006). Certain densities and thicknesses of the boundary layer have been modeled to cause strongly variable plumes pulsating with periods from a few million years. to more than 100 m.y. (Lin and Keken, 2006).

Global seismological tomography has revealed two large anomalously slow areas centered on roughly antipodal equatorial regions under Africa and the central Pacific (e.g., Gu et al., 2001). These anomalies are sometimes referred to as "superplumes," but this may be a misnomer if upwellings of this size and magnitude are not caused by Rayleigh-Taylor instabilities. In other words, in that case, they are not plumes sensu stricto. Many investigators have associated them with hotter than normal material rising from the thermal boundary layer near the core-mantle boundary (e.g., Courtillot et al., 2003; Torsvik et al., 2006). Most hotspots are

located near the edges of these lower-mantle anomalies, and edge-driven convection has been inferred as one mechanism to enhance the formation of plumes along their edges (Torsvik et al., 2006). All our studied hotspots, with the exception of Iceland and Yellowstone, are located within this zone, indicating that their origins are predominantly associated with the deepest mantle.

The "superplume" concept was first challenged by Anderson (1994), who noted the anticorrelation between the "superplumes" and subduction zones. He suggested that the regions in the African and Pacific mantle are hot because they have not been cooled or displaced by cold oceanic lithosphere for more than 200 m.y. This view later gained support, e.g., from Finn et al. (2005), who argued that the diffuse alkaline magmatic province encompassing the easternmost part of the Indo-Australian plate, West Antarctica, and the southwest portion of the Pacific plate was caused by slabs subducting in the Late Cretaceous, triggering lateral and vertical flow of warm Pacific mantle.

The African and Pacific mantle anomalies fail to meet several criteria inherent in standard plume theory, e.g., they are not related to a large plume head followed by narrow tail (for a review on the plume theory, see Campbell and Davies, 2006). We thus argue that the large mantle upwellings are an expression of return flow in Earth's mantle in response to subduction, spanning the whole mantle.

We recognize that the two mantle upwellings most likely extend downward to the core-mantle boundary, and it is unlikely that the two mantle upwellings co-pulsate without some kind of interaction with the core. We thus postulate that the apparent co-pulsations result from global fluctuations in such core-mantle interactions. This hypothesis implies periodic heating of Earth's core and subsequent heat release to the mantle and increased global plume activity from the edges of the lower-mantle anomalies. It should be noted that the co-pulsation of the two upwellings is evident also on longer time scales; they both expressed limited magmatism from ca. 100 to 50 Ma, but strong activity thereafter (Finn et al., 2005).

Nakagawa and Tackley (2005) modeled the thermal evolution of the core through geological time. Their most successful model, including 100 ppm radioactive potassium in the core, indicates fluctuations in the heat flow at the core-mantle boundary on the order of ± 10 TW. Herndon (2007), following a different approach, may have demonstrated the feasibility of a nuclear-fission chain reactor at the center of Earth's core. Herndon (2007) proposed a georeactor consisting of an inner subcore of actinide elements, sur-

rounded by a subshell with decay products. The energetic heat production would be expected to cause actinide subcore disassembly, mixing actinide elements with neutron absorbers of the subshell, and thus quenching the nuclear fission chain reaction. However, as actinide elements settled out of the mix, the chain reaction would restart (Herndon, 2009). The system might stabilize, or it might lead to fluctuating heat production. The frequency of fluctuations we observe (10 m.y. time scale) is not yet resolvable in the unconfirmed models of Nakagawa and Tackley (2005) and Herndon (2009), but we speculate that they may be present.

Significant lateral flow has been proposed for many hotspots, e.g., lateral sublithospheric flow of more than 1500 km has been inferred from the Canary hotspot eastward into North Africa (Duggen et al., 2009). Our hypothesis relates core pulsations to surface pulses in magmatism. If correct, this hypothesis implies dominantly near-vertical ascent of plume material, and relatively uniform rheology along the edges of the lower-mantle anomalies.

We do not infer that all magmatism discussed here is directly related to mantle plumes. For instance, the large amplitude of the North Atlantic magmatism around continental breakup at ca. 53 Ma was most likely related to interaction between the Iceland plume and breakup processes (Mjelde and Faleide, 2009). Another example concerns the (nonplume) silicic volcanism in Afar at 10 Ma (Kieffer et al., 2004). Our observations may suggest that the intensity of hotspots is modulated by fluctuations in plumes originating from the lower mantle.

CONCLUSIONS

We have reviewed studies of Earth's most significant intraplate Cenozoic hotspots (omitting the Holocene), with regard to variations in magmatic productivity through time. The study includes Pacific, Atlantic, and Indian hotspots, as well as Afar-Kenya, Yellowstone, and European magmatism. The results indicate that the pattern of investigated magmatism is not randomly distributed in time. Primary magmatic peaks may be identified at 10 Ma, 22 Ma, 30 Ma, 40 Ma, 49 Ma, and 60 Ma, and secondary peaks at 4 Ma, 15 Ma, 34 Ma, 45 Ma, and 65 Ma. Spectral analysis seems to confirm a dominant period of ~10 m.y. and a secondary period around 5 m.y.

It is unlikely that the observed global variations in magmatic productivity can be explained by differences in lithospheric thickness, fluctuations in intraplate stress levels following plate-tectonic reorganizations, and/or interaction with spreading ridges. It is also unlikely

that the global co-pulsations can be related to stable solitary waves, which may form in plume conduits, or to plume separation effects at the 670 km discontinuity.

Global seismological tomography has revealed two large anomalously slow areas under Africa and the central Pacific, which we interpret as upwellings spanning the entire mantle. Most of the studied hotspots are located near the edges of these lower-mantle anomalies, indicating origins predominantly in the deepest mantle.

Models of the thermal evolution of Earth's core through geological time indicate fluctuations in the heat flow at the core-mantle boundary. It is postulated that the apparent co-pulsations in magmatism result from global fluctuations in core-mantle interaction, involving periodic heating of the core and subsequent heat release to the mantle and increased global plume activity from the edges of the lower-mantle anomalies.

While the data selection for this study is limited to published results, we note that the analysis of our expanded and truly global data set largely confirms the trends noted by Mjelde and Faleide (2009), which were derived solely from Hawaii and Iceland plume fluxes.

REFERENCES CITED

Adam, C., Vidal, V., and Bonneville, A., 2005, MiFil: A method to characterize seafloor swells with application to the south central Pacific: Geochemistry, Geophysics, Geosystems, v. 6, Q01003, doi: 10.1029/2004GC000814.
Adam, C., Vidal, V., and Escartín, J., 2007, 80-Myr history of buoyancy and volcanic fluxes along the trails of the Walvis and St. Helena hotspots (South Atlantic): Earth

and Planetary Science Letters, v. 261, p. 432–442, doi: 10.1016/j.epsl.2007.07.005.

Ancochea, E., Hernán, F., Huertas, M.J., Brändle, J.L., and Herrera, R., 2006, A new chronostratigraphical and evolutionary model for La Gomera: Implications for the overall evolution of the Canarian Archipelago: Journal of Volcanology and Geothermal Research, v. 157, p. 271–293, doi: 10.1016/j.jvolgeores.2006.04.001.

Anderson, D.L., 1994, Superplumes or supercontinents?: Geology, v. 22, p. 39–42, doi: 10.1130/0091-7613(1994)022<0039:SOS>2.3.CO;2.

Bastow, I.D., Nyblade, A.A., Stuart, G.W., Rooney, T.O., and Benoit, M.H., 2008, Upper mantle seismic structure beneath the Ethiopian hot spot: Rifting at the edge of the African low-velocity anomaly: Geochemistry, Geophysics, Geosystems, v. 9, Q12022, doi: 10.1029/2008GC002107.

Beccaluva, L., Bianchini, G., Natali, C., and Siena, F., 2009, Continental flood basalts and mantle plumes: A case study of the northern Ethiopian Plateau: Journal of Petrology, v. 50, p. 1377–1403, doi: 10.1093/petrology/egp024.

Becker, T.W., Conrad, C.P., Buffett, B., and Müller, R.D., 2009, Past and present seafloor age distributions and the temporal evolution of plate tectonic heat transport: Earth and Planetary Science Letters, v. 278, p. 233–242, doi: 10.1016/j.epsl.2008.12.007.

Bercovici, D., and Mahoney, J., 1994, Double flood basalts and plume separation at the 660-km discontinuity: Science, v. 266, p. 1367–1369, doi: 10.1126/science.266.5189.1367.

Bonneville, A., Von Herzen, R.P., and Lucazeau, F., 1997, Heat flow over Reunion hot spot track: Additional evidence for thermal rejuvenation of oceanic lithosphere: Journal of Geophysical Research, v. 102, p. 22,731–22,747, doi: 10.1029/97JB00952.

Breivik, A.J., Faleide, J.I., and Mjelde, R., 2008, Neogene magmatism northeast of the Aegir and Kolbeinsey Ridges, NE Atlantic; spreading ridge–mantle plume interaction?: Geochemistry, Geophysics, Geosystems, v. 9, Q02004, doi: 10.1029/2007GC001750.

Camacho, A.G., Fernández, J., González, P.J., Rundle, J.B., Prieto, J.F., and Arjona, A., 2009, Structural results for La Palma island using 3-D gravity inversion: Journal of Geophysical Research, v. 114, B05411, doi: 10.1029/2008JB005628.

Campbell, I.H., and Davies, G.F., 2006, Do mantle plumes exist?: Episodes, v. 29, p. 162–168.

Cande, S.C., and Kent, D.V., 1995, Revised calibration of the geomagnetic polarity timescale for the Late Cretaceous and Cenozoic: Journal of Geophysical Research, v. 100, no. B4, p. 6093–6095, doi: 10.1029/94JB03098.

Cannat, M., Briais, A., Deplus, C., Escartín, J., Georgen, J., Lin, J., Mercouriev, S., Meyzen, C., Muller, M., Pouliquen, G., Rabain, A., and da Silva, P., 1999, Mid-Atlantic Ridge—Azores hot spot interactions: Along-axis migration of a hot spot–derived magmatic pulse 14 to 4 m.y. ago: Earth and Planetary Science Letters, v. 173, p. 257–269, doi: 10.1016/S0012-821X(99)00234-4.

Carracedo, J.C., Rodríguez Badiola, E., Guillou, H., Paterne, M., Scaillet, S., Pérez Torrado, F.J., Paris, R., Fra-Paleo, U., and Hansen, A., 2007, Eruptive and structural history of Teide Volcano and rift zones of Tenerife: Canary Islands: Geological Society of America Bulletin, v. 119, p. 1027–1051, doi: 10.1130/B26087.1.

Charvis, P., Laesanpura, A., Gallart, J., Hirn, A., Lépine, J.-C., de Voogd, B., Minshull, T.A., Hello, Y., and Pontoise, B., 1999, Spatial distribution of hotspot material added to the lithosphere under la Réunion, from wide-angle seismic data: Journal of Geophysical Research, v. 104, p. 2875–2893, doi: 10.1029/98JB02841.

Cheng, Q.C., Macdougall, J.D., and Zhu, P., 1999, Isotopic constraints on the Easter Seamount chain source: Contributions to Mineralogy and Petrology, v. 135, p. 225–233, doi: 10.1007/s004100050508.

Chorowicz, J., 2005, The East African Rift system: Journal of African Earth Sciences, v. 43, p. 379–410, doi: 10.1016/j.jafrearsci.2005.07.019.

Clouard, V., and Bonneville, A., 2001, How many Pacific hotspots are fed by deep-mantle plumes?: Geology, v. 29, p. 695–698, doi: 10.1130/0091-7613(2001)029<0695:HMPHAF>2.0.CO;2.

Coffin, M.F., and Eldholm, O., 1994, Igneous provinces: Crustal structure, dimensions, and external consequences: Reviews of Geophysics, v. 32, p. 1–36, doi: 10.1029/93RG02508.

Coffin, M.F., Pringle, M.S., Duncan, R.A., Gladzenko, T.P., Storey, M., Müller, R.D., and Gahagan, L.A., 2002, Kerguelen hotspot magma output since 130 Ma: Journal of Petrology, v. 43, p. 1121–1139, doi: 10.1093/petrology/43.7.1121.

Cogné, J.-P., and Humler, E., 2006, Trends and rhythms in global seafloor generation rate: Geochemistry, Geophysics, Geosystems, v. 7, Q03011, doi: 10.1029/2005GC001148.

Corti, G., 2009, Continental rift evolution: From rift initiation to incipient break-up in the Main Ethiopian Rift, East Africa: Earth-Science Reviews, v. 96, p. 1–53, doi: 10.1016/j.earscirev.2009.06.005.

Coulié, E., Quidelleur, X., Gillot, P.Y., Coutillot, V., Lefevre, J.C., and Chiessa, S., 2003, Comparative K-Ar and Ar/Ar dating of Ethiopian and Yemenite Oligocene volcanism: Implication for timing and duration of the Ethiopian traps: Earth and Planetary Science Letters, v. 206, p. 477–492, doi: 10.1016/S0012-821X(02)01089-0.

Courtillot, V., Jaupart, C., Manighetti, I., Tapponnier, P., and Besse, J., 1999, On causal links between flood basalts and continental breakup: Earth and Planetary Science Letters, v. 166, p. 177–195, doi: 10.1016/S0012-821X(98)00282-9.

Courtillot, V., Davaille, A., Besse, J., and Stock, J., 2003, Three different types of hotspots in the Earth's mantle: Earth and Planetary Science Letters, v. 205, p. 295–308, doi: 10.1016/S0012-821X(02)01048-8.

Crough, S.T., 1978, Thermal origin of mid-plate hot-spot swells: Geophysical Journal of the Royal Astronomical Society, v. 55, p. 451–469.

Crough, S., 1983, Hotspot swells: Annual Review of Earth and Planetary Sciences, v. 11, p. 165–193, doi: 10.1146/annurev.ea.11.050183.001121.

Detrick, R.S., Needham, H.D., and Renard, V., 1995, Gravity anomalies and crustal thickness variations along the Mid-Atlantic Ridge between 33°N and 40°N: Journal of Geophysical Research, v. 100, p. 3767–3787, doi: 10.1029/94JB02649.

Detrick, R.S., Sinton, J.M., Ito, G., Canales, J.P., Behn, M., Blacic, T., Cushman, B., Dixon, J.E., Graham, D.W., and Mahoney, J.J., 2002, Correlated geophysical, geochemical, and volcanological manifestations of plume-ridge interaction along the Galápagos spreading center: Geochemistry, Geophysics, Geosystems, v. 3, 8501, doi: 10.1029/2002GC000350.

Doucet, S., Scoates, J.S., Weis, D., and Giret, A., 2005, Constraining the components of the Kerguelen mantle plume: A Hf-Pb-Sr-Nd isotopic study of picrites and high-MgO basalts from the Kerguelen Archipelago: Geochemistry, Geophysics, Geosystems, v. 6, Q04007, doi: 10.1029/2004GC000806.

Duggen, S., Hoernle, K.A., Hauff, F., Klügel, A., Bouabdellah, M., and Thirlwall, M.F., 2009, Flow of Canary mantle plume material through a subcontinental lithospheric corridor beneath Africa to the Mediterranean: Geology, v. 37, p. 283–286, doi: 10.1130/G25426A.1.

Duncan, R., 1978, Geochronology of basalts from the Nine-tyeast Ridge and continental dispersion in the Eastern Indian Ocean: Journal of Volcanology and Geothermal Research, v. 4, p. 283–305, doi: 10.1016/0377-0273(78)90018-5.

Duncan, R.A., and McDougall, I., 1976, Linear volcanism in French Polynesia: Journal of Volcanology and Geothermal Research, v. 1, p. 197–227, doi: 10.1016/0377-0273(76)90008-1.

Duncan, R.A., and Storey, M., 1992, The life cycle of the Indian Ocean, in Duncan, R.A., Rea, D.K., Kidd, R.B., von Rad, U., and Weissel, J.K., eds., Synthesis of Results from Scientific Drilling in the Indian Ocean: American Geophysical Union Geophysical Monograph 70, p. 91–103.

Duncan, R.A., Backman, J., and McDonald, A., 1989, Reunion hotspot activity through Tertiary time: Initial Results from Ocean Drilling Program, Leg 115: Journal of Volcanology and Geothermal Research, v. 36, p. 193–198, doi: 10.1016/0377-0273(89)90013-9.

Eldholm, O., Thiede, J., and Taylor, E., 1989, Evolution of the Vøring volcanic margin, in Proceedings of the Ocean Drilling Program, Scientific Results, Volume 104: College Station, Texas, Ocean Drilling Program, p. 1033–1065.

Elliott, G.M., Berndt, C., and Parson, L.M., 2009, The SW African volcanic rifted margin and the initiation of the Walvis Ridge, South Atlantic: Marine Geophysical Researches, v. 30, p. 207–214, doi: 10.1007/s11001-009-9077-x.

Feraud, G., Giannerini, G., Campredon, R., and Stillman, C.J., 1985, Geochronology of some Canarian dike swarms: Contribution to the volcano-tectonic evolution of the archipelago: Journal of Volcanology and Geothermal Research, v. 25, p. 29–52, doi: 10.1016/0377-0273(85)90003-4.

Finn, C.A., Müller, R.D., and Panter, K.S., 2005, A Cenozoic diffuse alkaline magmatic province (DAMP) in the southwest Pacific without rift or plume origin: Geochemistry, Geophysics, Geosystems, v. 6, Q02005, doi: 10.1029/2004GC000723.

Fitton, J.G., Mahoney, J.J., Wallace, P.J., and Saunders, A.D., 2004, Origin and evolution of the Ontong Java Plateau: Introduction, in Fitton, J.G., Mahoney, J.J., Wallace, P.J., and Saunders, A.D., Origin and Evolution of the Ontong Java Plateau: Geological Society, London, Special Publication 229, p. 1–8, doi: 10.1144/GSL.SP.2004.229.01.01.

Furman, T., Bryce, J., Rooney, T., Hanan, B., Yirgu, G., and Ayalew, D., 2006, Heads and tails: 30 million years of Afar plume, in Yirgu, G., Ebinger, C.J., and Maguire, P.K.H., eds., The Afar Volcanic Province within the East African Rift system: Geological Society, London, Special Publication 259, p. 95–119.

Geldmacher, J., Hoernle, K., van den Bogaard, P., Zankl, G., and Garbe-Schönberg, D., 2001, Earlier history of the ≥70 Ma old Canary hotspot based on the temporal and geochemical evolution of the Selvagen archipelago and neighboring seamounts in the eastern North Atlantic: Journal of Volcanology and Geothermal Research, v. 111, p. 55–87, doi: 10.1016/S0377-0273(01)00220-7.

Geldmacher, J., Hanan, B.B., Blichert-Toft, J., Harpp, K., Hoernle, K., Hauff, F., Werner, R., and Kerr, A.C., 2003, Hafnium isotopic variations in volcanic rocks from the Caribbean large igneous province and Galápagos hot spot tracks: Geochemistry, Geophysics, Geosystems, v. 4, 1062, doi: 10.1029/2002GC000477.

Geldmacher, J., Hoernle, K., Bogaard, P.d., Duggen, S., and Werner, R., 2005, New ^{40}Ar/^{39}Ar age and geochemical data from seamounts in the Canary and Madeira volcanic provinces: Support for the mantle plume hypothesis: Earth and Planetary Science Letters, v. 237, p. 85–101, doi: 10.1016/j.epsl.2005.04.037.

Geldmacher, J., Hoernle, K., Klügel, A., Bogaard, P.d., Wombacher, F., and Berning, B., 2006, Origin and geochemical evolution of the Madeira-Tore Rise (eastern North Atlantic): Journal of Geophysical Research, v. 111, B09206, doi: 10.1029/2005JB003931.

Gente, G., Dyment, J., Maia, M., and Goslin, J., 2003, Interaction between the Mid-Atlantic Ridge and the Azores hot spot during the last 85 Myr: Emplacement and rifting of the hot spot–derived plateaus: Geochemistry, Geophysics, Geosystems, v. 4, 8514, doi: 10.1029/2003GC000527.

George, R., Rogers, N., and Kelley, S., 1998, Earliest magmatism in Ethiopia: Evidence for two mantle plumes in one flood basalt province: Geology, v. 26, p. 923–926, doi: 10.1130/0091-7613(1998)026<0923:EMIEEF>2.3.CO;2.

Gripp, A.E., and Gordon, R.G., 2002, Young tracks of hotspots and current plate velocities: Geophysical Journal International, v. 150, p. 321–361, doi: 10.1046/j.1365-246X.2002.01627.x.

Gu, Y.J., Dziewonski, A.M., Su, W.J., and Ekstrom, G., 2001, Models of the mantle shear velocity and discontinuities in the pattern of lateral heterogeneities: Journal of Geophysical Research, v. 106, p. 11,169–11,199, doi: 10.1029/2001JB000340.

Guillou, H., Maury, R.C., Blais, S., Cotten, J., Legendre, C., Guille, G., and Caroff, M., 2005, Age progression along the Society hotspot chain (French Polynesia) based on new unspiked K-Ar ages: Bulletin de la Societé Geologique Francaise, v. 176, p. 135–150, doi: 10.2113/176.2.135.

Gutiérrez, M., Casillas, R., Fernández, C., Balogh, K., Ahijado, A., Castillo, C., Colmenero, J.R., and García-

Navarro, E., 2006, The submarine volcanic succession of the basal complex of Fuerteventura, Canary Islands: A model of submarine growth and emergence of tectonic volcanic islands: Geological Society of America Bulletin, v. 118, p. 785–804, doi: 10.1130/B25821.1.

Haase, K.M., Mertz, D.F., Sharp, W.S., and Garbe-Schönberg, C.-D., 2000, Sr-Nd-Pb isotope ratios, geochemical compositions, $^{40}Ar/^{39}Ar$ data of lavas from San Felix Island (southeast Pacific): Implications for magma genesis and sources: Terra Nova, v. 12, p. 90–96.

Hart, S.R., Coetzee, M., Workman, R.K., Blusztajn, J., Johnson, K.T.M., Sinton, J.M., Steinberger, B., and Hawkins, J.W., 2004, Genesis of the Western Samoa seamount province: Age, geochemical fingerprint and tectonics: Earth and Planetary Science Letters, v. 227, p. 37–56, doi: 10.1016/j.epsl.2004.08.005.

Hawkins, J.W., and Natland, J.H., 1975, Nephelinites and basanites of the Samoan linear volcanic chain: Their possible tectonic significance: Earth and Planetary Science Letters, v. 24, p. 427–439, doi: 10.1016/0012-821X(75)90150-8.

Herndon, J.M., 2007, Nuclear georeactor generation of Earth's geomagnetic field: Current Science, v. 93, p. 1485–1487.

Herndon, J.M., 2009, Nature of planetary matter and magnetic field generation in the solar system: Current Science, v. 96, p. 1033–1039.

Hey, R., Martinez, F., and Höskuldsson, A., 2010, Propagating rift model for the V-shaped ridges south of Iceland: Geochemistry, Geophysics, Geosystems, v. 11, Q03011, doi: 10.1029/2009GC002865.

Hieronymus, C.F., and Bercovici, D., 2001, A theoretical model of hotspot volcanism: Control on volcanic spacing and patterns via magma dynamics and lithospheric stresses: Journal of Geophysical Research, v. 106, p. 683–702, doi: 10.1029/2000JB900355.

Hillier, J.K., 2007, Pacific seamount volcanism in space and time: Geophysical Journal International, v. 168, p. 877–889, doi: 10.1111/j.1365-246X.2006.03250.x.

Hoernle, K.A.J., and Schmincke, H.-U., 1993, The role of partial melting in the 15-Ma geochemical evolution of Gran Canaria: A blob model for the Canary hotspot: Journal of Petrology, v. 34, p. 599–626.

Hoernle, K., van den Bogaard, P., Werner, R., Lissina, B., Hauff, F., Alvarado, G., and Garbe-Schönberg, D., 2002, Missing history (16–71 Ma) of the Galapagos hotspot: Implications for the tectonic and biological evolution of the Americas: Geology, v. 30, p. 795–798, doi: 10.1130/0091-7613(2002)030<0795:MHMOTG>2.0.CO;2.

Hofmann, C., Courtillot, V., Féraud, G., Rochette, P., Yirgu, G., Ketefo, E., and Pik, R., 1997, Timing of the Ethiopian flood basalt event and implications for plume birth and global change: Nature, v. 389, p. 838–841, doi: 10.1038/39853.

Holbrook, W.S., Larsen, H.C., Korenaga, J., Dahl-Jensen, T., Reid, I.D., Kelemend, P.B., Hopper, J.R., Kente, G.M., Lizarralde, D., Bernstein, S., and Detrick, R.S., 2001, Mantle thermal structure and active upwelling during continental breakup in the North Atlantic: Earth and Planetary Science Letters, v. 190, p. 251–266, doi: 10.1016/S0012-821X(01)00392-2.

Holm, P.M., Grandvuinet, T., Friis, J., Wilson, J.R., Barker, A.K., and Plesner, S., 2008, An $^{40}Ar-^{39}Ar$ study of the Cape Verde hot spot: Temporal evolution in a semi-stationary plate environment: Journal of Geophysical Research, v. 113, B08201, doi: 10.1029/2007JB005339.

Ingle, S., Weis, D., Doucet, S., and Mattielli, N., 2003, Hf isotope constraints on mantle sources and shallow-level contaminants during Kerguelen hot spot activity since <120 Ma: Geochemistry, Geophysics, Geosystems, v. 4, 1068, doi: 10.1029/2002GC000482.

Ito, G., 2001, Reykjanes 'V'-shaped ridges originating from a pulsing and dehydrating mantle plume: Nature, v. 411, p. 681–684, doi: 10.1038/35079561.

Jiménez-Munt, I., Fernandez, M., Torné, M., and Bird, P., 2001, The transition from linear to diffuse plate boundary in the Azores-Gibraltar region: Results from a thin-sheet model: Earth and Planetary Science Letters, v. 192, p. 175–189, doi: 10.1016/S0012-821X(01)00442-3.

Kieffer, B., Arndt, N., Lapierre, H., Bastien, F., Bosch, D., Pecher, A., Yirgu, G., Yalew, D.E., Weis, D., Jerram, D.A., Keller, F., and Meugniot, C., 2004, Flood and shield basalts from Ethiopia: Magmas from the Afri-

can superswell: Journal of Petrology, v. 45, p. 793–834, doi: 10.1093/petrology/egg112.

Knesel, K.M., Cohen, B.E., Vasconcelos, P.M., and Thiede, D.S., 2008, Rapid change in drift of the Australian plate records collision with Ontong Java plateau: Nature, v. 454, p. 754–757, doi: 10.1038/nature07138.

Koppers, A.A.P., Duncan, R.A., and Steinberger, B., 2004, Implications of a nonlinear $^{40}Ar/^{39}Ar$ age progression along the Louisville seamount trail for models of fixed and moving hot spots: Geochemistry, Geophysics, Geosystems, v. 5, Q06L02, doi: 10.1029/2003GC000671.

Koppers, A.A.P., Russell, J.A., Jackson, M.G., Konter, J., Staudigel, H., and Hart, S.R., 2008, Samoa reinstated as a primary hotspot trail: Geology, v. 36, p. 435–438, doi: 10.1130/G24630A.1.

Krienitz, M.-S., Haase, K.M., Bogaard, P.d., Thiemann, V., and Shaikh-Mashail, M.A., 2009, Tectonic events, continental intraplate volcanism, and mantle plume activity in northern Arabia: Constraints from geochemistry and Ar-Ar dating of Syrian lavas: Geochemistry, Geophysics, Geosystems, v. 10, Q04008, doi: 10.1029/2008GC002254.

Kroenke, L.W., Wessel, P., and Sterling, A., 2004, Motion of the Ontong Java Plateau in the hot-spot frame of reference: 122 Ma–present, *in* Fitton, J.G., Mahoney, J.J., Wallace, P.J., and Saunders, A.D., eds., Origin and Evolution of the Ontong Java Plateau: Geological Society, London, Special Publication 229, p. 9–20.

Lawver, L.A., and Müller, R.D., 1994, Iceland hotspot track: Geology, v. 22, p. 311–314, doi: 10.1130/0091-7613(1994)022<0311:IHT>2.3.CO;2.

Lin, S.-C., and van Keken, P.E., 2006, Dynamics of thermochemical plumes: 2. Complexity of plume structures and its implications for mapping mantle plumes: Geochemistry, Geophysics, Geosystems, v. 7, Q03003, doi: 10.1029/2005GC001072.

Lodge, A., and Helffrich, G., 2006, Depleted swell root beneath the Cape Verde Islands: Geology, v. 34, p. 449–452, doi: 10.1130/G22030.1.

Longpré, M.-A., Troll, V.R., and Hansteen, T.H., 2008, Upper mantle magma storage and transport under a Canarian shield-volcano, Teno, Tenerife (Spain): Journal of Geophysical Research, v. 113, B08203, doi: 10.1029/2007JB005422.

Lonsdale, P., 1988, Geography and history of the Louisville hotspot chain in the southern Pacific: Journal of Geophysical Research, v. 93, p. 3078–3104, doi: 10.1029/JB093iB04p03078.

Lonsdale, P., and Klitgord, K.D., 1978, Structure and tectonic history of the Eastern Panama Basin: Geological Society of America Bulletin, v. 89, p. 981–999, doi: 10.1130/0016-7606(1978)89<981:SATHOT>2.0.CO;2.

Luais, B., 2004, Temporal changes in Nd isotopic composition of Piton de la Fournaise magmatism (Réunion Island, Indian Ocean): Geochemistry, Geophysics, Geosystems, v. 5, Q01008, doi: 10.1029/2002GC000502.

Lustrino, M., and Wilson, M., 2007, The circum-Mediterranean anorogenic Cenozoic igneous province: Earth-Science Reviews, v. 81, p. 1–65, doi: 10.1016/j.earscirev.2006.09.002.

Marcaillou, B., Charvis, P., and Collot, J.-Y., 2006, Structure of the Malpelo Ridge (Colombia) from seismic and gravity modelling: Marine Geophysical Researches, v. 27, p. 289–300, doi: 10.1007/s11001-006-9009-y.

McDougall, I., and Schmincke, H.-U., 1976, Geochronology of Gran Canaria, Canary Islands: Age of shield building volcanism and other magmatic phases: Bulletin of Volcanology, v. 40, p. 1–21.

Meco, J., Scaillet, S., Guillou, H., Lomoschitz, A., Carracedo, J.C., Ballester, J., Betancort, J.-F., and Cilleros, A., 2007, Evidence for long-term uplift on the Canary Islands from emergent Mio–Pliocene littoral deposits: Global and Planetary Change, v. 57, p. 222–234, doi: 10.1016/j.gloplacha.2006.11.040.

Menéndez, I., Silva, P.G., Martín-Betancor, M., Pérez-Torrado, F.J., Guillou, H., and Scaillet, S., 2008, Fluvial dissection, isostatic uplift, and geomorphological evolution of volcanic islands (Gran Canaria, Canary Islands, Spain): Geomorphology, v. 102, p. 189–203, doi: 10.1016/j.geomorph.2007.06.022.

Meshesha, D., and Shinjo, R., 2008, Rethinking geochemical features of the Afar and Kenya mantle plumes and

geodynamic implications: Journal of Geophysical Research, v. 113, B09209, doi: 10.1029/2007JB005549.

Michon, L., Saint-Ange, F., Bachelery, P., Villeneuve, N., and Staudacher, T., 2007, Role of the structural inheritance of the oceanic lithosphere in the magmato-tectonic evolution of Piton de la Fournaise volcano (La Réunion Island): Journal of Geophysical Research, v. 112, B04205, doi: 10.1029/2006JB004598.

Mjelde, R., and Faleide, J.I., 2009, Variation of Icelandic and Hawaiian magmatism: evidence for co-pulsation of mantle plumes?: Marine Geophysical Researches, v. 30, p. 61–72, doi: 10.1007/s11001-009-9066-0.

Mjelde, R., Breivik, A.J., Raum, T., Mittelstaedt, E., Ito, G., and Faleide, J.I., 2008, Magmatic and tectonic evolution of the North Atlantic: Journal of the Geological Society of London, v. 165, p. 31–42, doi: 10.1144/0016-76492007-018.

Mjelde, R., Faleide, J.I., Breivik, A.J., and Raum, T., 2009, Lower crustal composition and crustal lineaments on the Vøring margin, NE Atlantic: A review: Tectonophysics, v. 472, p. 183–193, doi: 10.1016/j.tecto.2008.04.018.

Montelli, R., Nolet, G., Dahlen, F.A., Masters, G., Engdahl, E.R., and Hung, S.-H., 2004, Finite-frequency tomography reveals a variety of plumes in the mantle: Science, v. 303, p. 338–343, doi: 10.1126/science.1092485.

Morgan, W.J., 1971, Convection plumes in the lower mantle: Nature, v. 230, p. 42–43, doi: 10.1038/230042a0.

Morgan, W.J., 1972, Deep mantle convection plumes and plate motions: The American Association of Petroleum Geologists Bulletin, v. 56, p. 203–213.

Müller, R.D., Royer, J.-Y., and Lawver, L.A., 1993, Revised plate motions relative to the hotspots from combined Atlantic and Indian Ocean hotspot tracks: Geology, v. 21, p. 275–278, doi: 10.1130/0091-7613(1993)021<0275:RPMRTT>2.3.CO;2.

Nakagawa, T., and Tackley, P.J., 2005, Deep mantle heat flow and thermal evolution of the Earth's core in thermochemical multiphase models of mantle convection: Geochemistry, Geophysics, Geosystems, v. 6, Q08003, doi: 10.1029/2005GC000967.

Nicolaysen, K., Frey, F.A., Hodges, K.V., Weis, D., and Giret, A., 2000, $^{40}Ar-^{39}Ar$ geochronology of flood basalts from the Kerguelen Archipelago, southern Indian Ocean: Implications for Cenozoic eruption rates of the Kerguelen plume: Earth and Planetary Science Letters, v. 174, p. 313–328, doi: 10.1016/S0012-821X(99)00271-X.

O'Connor, J.M., and Duncan, R.A., 1990, Evolution of the Walvis Ridge–Rio Grande Rise hot spot system: Implications for African and South America plate motions over plumes: Journal of Geophysical Research, v. 95, p. 17,475–17,502, doi: 10.1029/JB095iB11p17475.

O'Connor, J.M., and le Roex, A.P., 1992, South Atlantic hot spot plume systems: 1. Distribution of volcanism in time and space: Earth and Planetary Science Letters, v. 113, p. 17,343–17,364.

O'Connor, J.M., Stoffers, P., and McWilliams, M.O., 1995, Time-space mapping of Easter Chain volcanism: Earth and Planetary Science Letters, v. 136, p. 197–212, doi: 10.1016/0012-821X(95)00176-D.

Olson, P., and Christensen, U., 1986, Solitary wave propagation in a fluid conduit within a viscous matrix: Journal of Geophysical Research, v. 91, p. 6367–6374.

Orihashi, Y., Al-Jailani, A., and Naga, K., 1998, Dispersion of the Afar plume: Implications from the spatiotemporal distribution of the late Miocene to Recent volcanics, southwestern Arabian Peninsula: Gondwana Research, v. 1, p. 221–234, doi: 10.1016/S1342-937X(05)70833-9.

Paris, R., Guillou, H., Carracedo, J.C., and Pérez-Torrado, F.J., 2005, Volcanic and morphological evolution of La Gomera (Canary Islands), based on new K-Ar ages and magnetic stratigraphy: Implications for oceanic island evolution: Journal of the Geological Society of London, v. 162, p. 501–512, doi: 10.1144/0016-764904-055.

Park, Y., Nyblade, A.A., Rodgers, A.J., and Al-Amri, A., 2007, Upper mantle structure beneath the Arabian Peninsula and northern Red Sea from teleseismic body wave tomography: Implications for the origin of Cenozoic uplift and volcanism in the Arabian Shield: Geochemistry, Geophysics, Geosystems, v. 8, Q06021, doi: 10.1029/2006GC001566.

Patriat, M., and Labails, C., 2006, Linking the Canary and Cape Verde hot-spots, northwest Africa: Marine

Geophysical Researches, v. 27, p. 201–215, doi: 10.1007/s11001-006-9000-7.

Paul, D., White, W.M., and Blichert-Toft, J., 2005, Geochemistry of Mauritius and the origin of rejuvenescent volcanism on oceanic island volcanoes: Geochemistry, Geophysics, Geosystems, v. 6, Q06007, doi: 10.1029/2004GC000883.

Petterson, M.G., Babbs, T., Neal, C.R., Mahoney, J.J., Saunders, A.D., Duncan, R.A., Tolia, D., Magua, R., Qopoto, C., Mahoaa, H., and Natogga, D., 1999, Geological–tectonic framework of Solomon Islands, SW Pacific: Crustal accretion and growth within an intra-oceanic setting: Tectonophysics, v. 301, p. 35–60, doi: 10.1016/S0040-1951(98)00214-5.

Plesner, S., Holm, P.M., and Wilson, J.R., 2003, $^{40}Ar/^{39}Ar$ geochronology of Santo Antão: Cape Verde Islands: Journal of Volcanological and Geothermal Research, v. 120, p. 103–121, doi: 10.1016/S0377-0273(02)00367-0.

Rabinowitz, P.D., and LaBrecque, J., 1979, The Mesozoic South Atlantic Ocean and evolution of its continental margins: Journal of Geophysical Research, v. 84, p. 5973–6002, doi: 10.1029/JB084iB11p05973.

Renne, P.R., WoldeGabriel, G., Hart, W.K., Heiken, G., and White, T.D., 1999, Chronostratigraphy of the Miocene–Pliocene Sagantole Formation, Middle Awash Valley, Afar rift, Ethiopia: Geological Society of America Bulletin, v. 111, p. 869–885, doi: 10.1130/0016-7606(1999)111<0869:COTMPS>2.3.CO;2.

Ritsema, J., van Heijst, H.J., and Woodhouse, J.H., 1999, Complex shear wave velocity structure imaged beneath Africa and Iceland: Science, v. 286, p. 1925–1928, doi: 10.1126/science.286.5446.1925.

Ritter, J.R.R., Jordan, M., Christensen, U.R., and Achauer, U., 2001, A mantle plume below the Eifel volcanic fields, Germany: Earth and Planetary Science Letters, v. 186, p. 7–14, doi: 10.1016/S0012-821X(01)00226-6.

Rogers, N., Macdonald, R., Fitton, J.G., George, R., Smith, M., and Barreiro, B., 2000, Two mantle plumes beneath the East African rift system: Sr, Nd and Pb isotope evidence from Kenya Rift basalts: Earth and Planetary Science Letters, v. 176, p. 387–400, doi: 10.1016/S0012-821X(00)00012-1.

Sallarès, V., Charvis, P., Flueh, E.R., and Bialas, J., 2003, Seismic structure of Cocos and Malpelo volcanic ridges and implications for hotspot-ridge interaction: Journal of Geophysical Research, v. 108, 2564, doi: 10.1029/2003JB002431.

Sandwell, D.T., and Smith, W.H.F., 1997, Marine gravity anomaly from Geosat and ERS 1 satellite altimetry: Journal of Geophysical Research, v. 102, p. 10,039–10,054, doi: 10.1029/96JB03223.

Schilling, J.G., 1975, Azores mantle blob: Rare-earth evidence: Earth and Planetary Science Letters, v. 25, p. 103–115, doi: 10.1016/0012-821X(75)90186-7.

Schirnick, C., Bogaard, P.d., and Schmincke, H.-U., 1999, Cone sheet formation and intrusive growth of an oceanic island—The Miocene Tejeda complex on Gran Canaria (Canary Islands): Geology, v. 27, p. 207–210, doi: 10.1130/0091-7613(1999)027<0207:CSFAIG>2.3.CO;2.

Schmincke, H.U., and Sumita, M., 1998, Volcanic evolution of Gran Canaria reconstructed from apron sediments. Synthesis VICAP drilling project (ODP Leg 157), in Weaver, P.P.E., Schmincke, H.U., Firth, J.V., Duffield, W., et al., Proceedings of the Ocean Drilling Program, Scientific Results, Volume 157: College Station, Texas, Ocean Drilling Program, p. 443–469.

Schutt, D.L., Dueker, K., and Yuan, H., 2008, Crust and upper mantle velocity structure of the Yellowstone hot spot

and surroundings: Journal of Geophysical Research, v. 113, B03310, doi: 10.1029/2007JB005109.

Seton, M., Gaina, C., Müller, R.D., and Heine, C., 2009, Mid-Cretaceous seafloor spreading pulse: Fact or fiction?: Geology, v. 37, p. 687–690, doi: 10.1130/G25624A.1.

Sims, K.W.W., Hart, S.R., Reagan, M.K., Blusztajn, J., Staudigel, H., Sohn, R.A., Layne, G.D., Ball, L.A., and Andrews, J., 2008, ^{238}U-^{230}Th-^{226}Ra-^{210}Pb-^{210}Po, ^{232}Th-^{228}Ra, and ^{235}U-^{231}Pa constraints on the ages and petrogenesis of Vailulu'u and Malumalu lavas, Samoa: Geochemistry, Geophysics, Geosystems, v. 9, Q04003, doi: 10.1029/2007GC001651.

Stachnik, J.C., Dueker, K., Schutt, D.L., and Yuan, H., 2008, Imaging Yellowstone plume-lithosphere interactions from inversion of ballistic and diffusive Rayleigh wave dispersion and crustal thickness data: Geochemistry, Geophysics, Geosystems, v. 9, Q06004, doi: 10.1029/2008GC001992.

Steinberger, B., 2000, Plumes in a convecting mantle: Models and observations for individual hotspots: Journal of Geophysical Research, v. 105, p. 11,127–11,152, doi: 10.1029/1999JB900398.

Stillman, C.J., Fuster, J.M., Bennell-Baker, M.J., Muñoz, M., Smewing, J.D., and Sagredo, J., 1975, Basal complex of Fuerteventura (Canary Islands) is an oceanic intrusive complex with rift-system affinities: Nature, v. 257, p. 469–471, doi: 10.1038/257469a0.

Todal, A., and Edholm, O., 1998, Continental margin off western India and Deccan large igneous province: Marine Geophysical Researches, v. 20, p. 273–291, doi: 10.1023/A:1004640508371.

Torsvik, T.H., and Cocks, L.R.M., 2005, Norway in space and time: A centennial cavalcade: Norwegian Journal of Geology, v. 85, p. 73–86.

Torsvik, T.H., Smethurst, M.A., Burke, K., and Steinberger, B., 2006, Large igneous provinces generated from the margins of the large low-velocity provinces in the deep mantle: Geophysical Journal International, v. 167, p. 1447–1460, doi: 10.1111/j.1365-246X.2006.03158.x.

Uto, U., Yamamoto, Y., Sudo, M., Uchiumi, S., Ishizuka, O., Kogiso, T., and Tsunakawa, H., 2007, New K-Ar ages of the Society Islands, French Polynesia, and implications for the Society hotspot feature: Earth, Planets, and Space, v. 59, p. 879–885.

Van Ark, E., and Lin, J., 2004, Time variation in igneous volume flux of the Hawaii-Emperor hot spot seamount chain: Journal of Geophysical Research, v. 109, B11401, doi: 10.1029/2003JB002949.

van Wijk, J.W., Huismans, R.S., Voorde, M.T., and Cloetingh, S.A.P.L., 2001, Melt generation at volcanic continental margins: No need for a mantle plume?: Geophysical Research Letters, v. 28, p. 3995–3998, doi: 10.1029/2000GL012848.

Verzhbitsky, E.V., 2003, Geothermal regime and genesis of the Ninety-East and Chagos-Laccadive ridges: Journal of Geodynamics, v. 35, p. 289–302, doi: 10.1016/S0264-3707(02)00068-6.

Vidal, V., and Bonneville, A., 2004, Variations of the Hawaiian hot spot activity revealed by variations in the magma production rate: Journal of Geophysical Research, v. 109, B03104, doi: 10.1029/2003JB002559.

Vlastélic, I., and Dosso, L., 2005, Initiation of a plume-ridge interaction in the South Pacific recorded by high-precision Pb isotopes along Hollister Ridge: Geochemistry, Geophysics, Geosystems, v. 6, Q05011, doi: 10.1029/2004GC000902.

Vlastélic, I., Dosso, L., Guillou, H., Bougault, H., Géli, L., Etoubleau, J., and Joron, J.L., 1998, Geochemistry of

the Hollister Ridge: Relation with the Louisville hotspot and the Pacific-Antarctic Ridge: Earth and Planetary Science Letters, v. 160, p. 777–793, doi: 10.1016/S0012-821X(98)00127-7.

Vogt, P.R., 1971, Asthenospheric motion recorded by the ocean floor south of Iceland: Earth and Planetary Science Letters, v. 13, p. 153–160, doi: 10.1016/0012-821X(71)90118-X.

Vogt, P.R., 1976, Plumes, subaxial pipe flow and topography along the mid-oceanic ridge: Earth and Planetary Science Letters, v. 29, p. 309–325, doi: 10.1016/0012-821X(76)90135-7.

Waite, G., Smith, R.B., and Allen, R.M., 2006, Vp and Vs structure of the Yellowstone hot spot upper mantle from teleseismic tomography: Evidence for an upper mantle plume: Journal of Geophysical Research, v. 111, B04303, doi: 10.1029/2005JB003867.

Wallace, P.J., Frey, F.A., Weis, D., and Coffin, M.F., 2002, Origin and evolution of the Kerguelen Plateau, Broken Ridge and Kerguelen Archipelago: Journal of Petrology, v. 43, p. 1105–1108, doi: 10.1093/petrology/43.7.1105.

Watts, A., Cochran, J., and Selzer, G., 1975, Gravity anomalies and flexure of the lithosphere: A three-dimensional study of the Great Meteor Seamount, northeast Atlantic: Journal of Geophysical Research, v. 80, p. 1391–1398, doi: 10.1029/JB080i011p01391.

Weis, D., Frey, F.A., Schlich, R., Schaming, M., Montigny, R., Damasceno, D., Mattielli, N., Nicolaysen, K.E., and Scoates, J.S., 2002, Trace of the Kerguelen mantle plume: Evidence from seamounts between the Kerguelen Archipelago and Heard Island: Indian Ocean: Geochemistry, Geophysics, Geosystems, v. 3, 1033, doi: 10.1029/2001GC000251.

Werner, R., Hoernle, K., Bogaard, P.d., Ranero, C.R., Huene, R., and Korich, D., 1999, Drowned 14-m.y.-old Galapagos archipelago off the coast of Costa Rica: Implications for tectonic and evolutionary models: Geology, v. 27, p. 499–502, doi: 10.1130/0091-7613(1999)027<0499:DMYOGP>2.3.CO;2.

Wessel, P., and Kroenke, L., 1997, A geometric technique for relocating hotspots and refining absolute plate motions: Nature, v. 387, p. 365–369, doi: 10.1038/387365a0.

Wessel, P., and Kroenke, L.W., 2008, Pacific absolute plate motion since 145 Ma: An assessment of the fixed hot spot hypothesis: Journal of Geophysical Research, v. 113, B06101, doi: 10.1029/2007JB005499.

White, R.S., 1993, Melt production rates in mantle plumes: Philosophical Transactions, Physical Sciences and Engineering, v. 342, p. 137–153, doi: 10.1098/rsta.1993.0010.

White, R.S., Brown, J.W., and Smallwood, J.R., 1995, The temperature of the Iceland plume and origin of outward propagating V-shaped ridges: Journal of the Geological Society of London, v. 152, p. 1039–1045.

Wilson, J.T., 1963, A possible origin of the Hawaiian Islands: Canadian Journal of Physics, v. 41, p. 863–870.

Xu, G., Frey, F.A., Weis, D., Scoates, J.S., and Giret, A., 2007, Flood basalts from Mt. Capitole in the central Kerguelen Archipelago: Insights into the growth of the archipelago and source components contributing to plume-related volcanism: Geochemistry, Geophysics, Geosystems, v. 8, Q06007, doi: 10.1029/2007GC001608.